

Accepted Manuscript

Human Colon Tumors Express a Dominant-negative Form of SIGIRR That Promotes Inflammation and Colitis-associated Colon Cancer in Mice

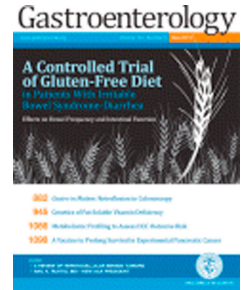
Junjie Zhao, Katarzyna Bulek, Muhammet Fatih Gulen, Jarod A. Zepp, Georgio Karagkounis, Bradley N. Martin, Hao Zhou, Minjia Yu, Xiuli Liu, Emina Huang, Paul L. Fox, Matthew F. Kalady, Sanford D. Markowitz, Xiaoxia Li

PII: S0016-5085(15)01258-5
DOI: [10.1053/j.gastro.2015.08.051](https://doi.org/10.1053/j.gastro.2015.08.051)
Reference: YGAST 60011

To appear in: *Gastroenterology*
Accepted Date: 24 August 2015

Please cite this article as: Zhao J, Bulek K, Gulen MF, Zepp JA, Karagkounis G, Martin BN, Zhou H, Yu M, Liu X, Huang E, Fox PL, Kalady MF, Markowitz SD, Li X, Human Colon Tumors Express a Dominant-negative Form of SIGIRR That Promotes Inflammation and Colitis-associated Colon Cancer in Mice, *Gastroenterology* (2015), doi: 10.1053/j.gastro.2015.08.051.

This is a PDF file of an unedited manuscript that has been accepted for publication. As a service to our customers we are providing this early version of the manuscript. The manuscript will undergo copyediting, typesetting, and review of the resulting proof before it is published in its final form. Please note that during the production process errors may be discovered which could affect the content, and all legal disclaimers that apply to the journal pertain.



Title: Human Colon Tumors Express a Dominant-negative Form of SIGIRR That Promotes Inflammation and Colitis-associated Colon Cancer in Mice

Short title: Inactivation of SIGIRR in colorectal cancer

Junjie Zhao^{1,3,7}, Katarzyna Bulek^{1,7}, Muhammet Fatih Gulen¹, Jarod A. Zepp^{1,3}, Georgio Karagkounis², Bradley N. Martin¹, Hao Zhou¹, Minjia Yu¹, Xiuli Liu⁴, Emina Huang^{2,5}, Paul L. Fox⁶, Matthew F. Kalady^{2,5}, Sanford D. Markowitz⁷, Xiaoxia Li¹.

1. Department of Immunology, Lerner Research Institute,
2. Department of stem cell biology and regenerative medicine, Lerner Research Institute,
3. Department of Molecular Medicine, Cleveland Clinic Lerner College of Medicine, Case Western Reserve University
4. Department of Anatomic Pathology
5. Department of Colorectal Surgery, Digestive Disease Institute,
6. Department of Cellular and Molecular Medicine, Lerner Research Institute
Cleveland Clinic Foundation, Cleveland, OH, USA;
7. Case Comprehensive Cancer Center,
Case Western Reserve University, Cleveland, OH, USA.
8. These authors contributed equally to this work.

Grant Support:

This study was supported by National Institutes of Health (P01 CA062220 to X.Li., P50CA150964 to S.D.M).

Correspondence:

Xiaoxia Li, Ph.D.

Department of Immunology,

Cleveland Clinic Foundation, 9500 Euclid Avenue, Cleveland, OH 44195, USA

E-mail: lix@ccf.org

Phone: (216) 445-8706

Fax: (216) 444-9329

Author contributions: X.Li conceived the study. J.Z., K.B. and X.Li designed the experiments. J.Z., K.B. performed most of the experiments. M.F.G., J.A.Z. assisted in data acquisition. H.Z., M.Y. provided technical support. X.L., M.F.K., E.H., P.L.F. and S.D.M. provided essential experimental material and participated in data interpretation. J.Z. and K.B., X.Li interpreted the data and prepared the manuscript.

Acknowledgement

The authors would like to thank Drs. Somasekar Seshagiri and Steffen Durinck at the Department of Molecular Biology of Genentech for providing the RNA sequencing data and preliminary analysis.

Conflicts of Interest

The authors declare no conflicts of interest.

Abstract

Background & Aims: Single immunoglobulin and toll-interleukin 1 receptor (SIGIRR), a negative regulator of the Toll-like and interleukin-1 receptor (IL1R) signaling pathways, controls intestinal inflammation and suppresses colon tumorigenesis in mice. However, the importance of SIGIRR in human colorectal cancer development has not been determined. We investigated the role of SIGIRR in development of human colorectal cancer.

Methods: We performed RNA sequence analyses of pairs of colon tumor and non-tumor tissues, each collected from 68 patients. Immunoblot and immunofluorescence analyses were used to determine levels of SIGIRR protein in primary human colonic epithelial cells, tumor tissues, and colon cancer cell lines. We expressed SIGIRR and mutant forms of the protein in Vaco cell lines. We created and analyzed mice that expressed full-length (control) or a mutant form of *Sigirr* (encoding SIGIRR^{N86/102S}, which is not glycosylated) specifically in the intestinal epithelium. Some mice were given azoxymethane and dextran sulfate sodium to induce colitis-associated cancer. Intestinal tissues were collected and analyzed by immunohistochemical and gene expression profile analyses.

Results: RNA sequence analyses revealed increased expression of a *SIGIRR* mRNA isoform, *SIGIRRΔE8*, in colorectal cancer tissues compared to paired non-tumor tissues. SIGIRRΔE8 is not modified by complex glycans and is therefore retained in the cytoplasm—it cannot localize to the cell membrane or reduce IL1R signaling. SIGIRRΔE8 interacts with and has a dominant-negative effect on SIGIRR, reducing its glycosylation, localization to the cell surface, and function. Most SIGIRR detected in human colon cancer tissues was cytoplasmic, whereas in non-tumor tissues it was found at the cell membrane. Mice that expressed SIGIRR^{N86/102S} developed more inflammation and formed larger tumors after administration of azoxymethane and dextran sulfate sodium than control mice; colon tissues from these mutant mice expressed higher levels of the inflammatory cytokines IL17A and IL6 had activation of the transcription factors STAT3 and NFκB. SIGIRR^{N86/102S} expressed in colons of mice did not localize to the epithelial cell surface.

Conclusion: Levels of SIGIRR are lower in human colorectal tumors, compared with non-tumor tissues; tumors contain the dominant-negative isoform SIGIRRΔE8. This mutant protein blocks localization of full-length SIGIRR to the surface of colon epithelial cells and its ability to downregulate IL1R signaling. Expression of SIGIRR^{N86/102S} in the colonic epithelium of mice increases expression of inflammatory cytokines and formation and size of colitis-associated tumors.

KEY WORDS: colon cancer, mouse model, tumor suppressor, AOM-DSS

Introduction

Colorectal carcinoma (CRC) is one of the leading causes of cancer-related mortality in the United States¹. The development of the CRCs exemplifies the multistep transformation model of tumorigenesis². They arise from mutational activation of oncogenes coupled with inactivation of tumor suppressor genes as a result of genomic instability². Somatic mutations accumulate in benign adenomas over time and with the influence from environmental factors such as inflammation, eventually lead to malignant transformation into carcinoma^{2,3}.

Inappropriate activation of toll-Interleukin-1receptor (TLR-IL-1R) signaling by commensal bacteria contributes to the pathogenesis of inflammatory bowel diseases and colitis-associated cancer^{4,5,6,7}. The single immunoglobulin interleukin 1 receptor related molecule (SIGIRR, also named TIR8) plays a critical role in modulating intestinal inflammation and suppressing colon tumorigenesis^{8,9}. SIGIRR is a unique member of the TLR-IL-1R superfamily, with a single immunoglobulin (Ig) extracellular domain and a TIR intracellular domain^{10,11}. SIGIRR is highly expressed in intestinal epithelial cells¹² and functions as a negative regulator for IL-1, IL-33, LPS and CpG signaling^{11,13}. We and others previously reported that SIGIRR-deficient mice are more susceptible to chemical induced colitis and exhibit increased tumorigenesis in the murine model of colitis-associated colon cancer^{12,14,15}. SIGIRR deficiency also leads to increased colon tumor burden in the *Apc^{Min}* mice¹⁶.

While previous studies have established SIGIRR as a suppressor of colon tumorigenesis in mice, the importance of SIGIRR in human colorectal cancer has not been determined. In this study, we found that SIGIRR is frequently inactivated in human colorectal cancer due to the expression of a dominant negative SIGIRR isoform. The SIGIRR isoform, SIGIRR^{ΔE8}, is encoded by a transcript lacking the exon 8 of the SIGIRR gene. SIGIRR^{ΔE8} showed increased retention in the cytoplasm and loss of complex glycan modification compared to the full-length SIGIRR, potentially due to its interaction with the endoplasmic reticulum (ER) resident protein RPN1(a subunit of oligosaccharyltransferase complex¹⁷). Moreover, SIGIRR^{ΔE8} was able to interact with full-length SIGIRR protein to sequester it from complex glycan modification and cell surface expression. RNA sequencing detected significant increased exclusion of exon8 in human colorectal cancer in a cohort of 68 pairs of normal and colon cancer samples. Consistently, human colon cancer showed predominantly cytoplasmic localization of SIGIRR in contrast to the cell membrane expression in normal tissue, potentially due to the dominant negative effect of SIGIRR^{ΔE8}. Consistently, using transgenic mice expressing a SIGIRR mutant bearing mutated glycosylation motif, we showed that loss of modification by complex glycan and lack of cell surface expression inactivated the tumor suppressor function of SIGIRR *in vivo*. In summary, our results suggest that the expression of a cancer-associated dominant negative SIGIRR isoform (SIGIRR^{ΔE8}) results in inactivation of SIGIRR function through increased ER retention, loss of appropriate glycosylation and cell surface expression, implicating SIGIRR as an important regulator of colorectal cancer in human.

Materials and Methods

Ethical Guidelines Collection and analysis of clinical samples (normal epithelium and colon cancer specimen) was approved by the Institutional Review Board of the Cleveland Clinic Foundation. The Institutional Animal Care and Use Committees of the Cleveland Clinic approved all animal experiments.

RNA sequencing analysis RNA sequencing analysis was performed on a previously described dataset¹⁸. The analysis of differential exon expression was based on RPKM values derived as previously described¹⁸. Analysis of junction reads was performed by aligning raw sequencing data with the Spliced Transcripts Alignment to a Reference (STAR)¹⁹ software followed by enumeration of individual read counts. Sequencing and genotype data are deposited at the European Genome-Phenome Archive (<http://www.ebi.ac.uk/ega/>), under accession number EGAS00001000288.

Biological reagents and cell culture. Recombinant human IL-1 β was purchased from R&D systems. Anti-HA and anti-FLAG (H3663) antibodies were purchased from Sigma-Aldrich. Anti-SIGIRR antibody used in immunostaining (HPA023188) was validated by the human protein atlas project and purchased from Sigma-Aldrich. Anti-SIGIRR antibody for western blot (AHP1784T) was all purchased from AbD Serotec. Anti-RPN1 (ab123904) and anti-Na⁺-K⁺ ATPase (ab58475) antibodies were purchased from Abcam. Human colon cancer tissue array was purchased from Abcam.

Detailed information on material and methods can be found in supplemental information section.

Results

Loss of N-linked glycosylation on SIGIRR in colorectal cancer. We examined SIGIRR expression in freshly isolated human colonic epithelial cells and tumor tissues together with a panel of colon cancer cell lines derived from different patients (VACO cell lines)^{20 21} by western blot. SIGIRR was detected as multiple bands ranging from 44kDa (size predicted based on full-length cDNA) to 90kDa in the normal colonic epithelial cells (**Fig. 1A and B**). Interestingly, the colon cancer cell lines and the colorectal cancer specimen showed a drastic reduction of the smear band above 55kDa and a concurrent increase of the bands migrating below 55kDa marker (**Fig. 1A and B**).

These observations prompted us to investigate what modification lead to the smear band of SIGIRR above 55kDa. Since SIGIRR is a transmembrane protein, we suspected that the modification in colonic epithelial cell-derived SIGIRR was due to N-linked glycosylation. Overexpressing human SIGIRR cDNA yielded highly modified forms of SIGIRR (**Fig. 2A**). There are four putative glycosylation motifs in the ectodomain of SIGIRR, which are conserved between mouse and human (**Fig. 2B**). We mutated the predicated sites by site-directed mutagenesis changing the asparagines to serines. Upon mutation of all of the 4 putative sites (SIGIRR^{N31/73/86/102S}), SIGIRR was reduced to the unmodified form 44kDa (**Fig. 2A**), confirming that SIGIRR is N-linked glycosylated protein. Moreover, PNGase F treatment of lysates from normal human colonic epithelial cells reduced the slow-migrating smear band to its predicted size (**Fig. 2C**), indicating the SIGIRR is N-linked glycosylated *in vivo*. The N-linked glycosylation is a multi-step process that starts in ER where the nascent protein acquires high-mannose modification and is transported to Golgi apparatus to receive further modification by complex glycan²². Based on the band pattern of SIGIRR, we hypothesized that the smear band that was reduced in the colon cancer cell lines, was due to complex glycan modification on SIGIRR. The complex glycan modification requires the enzymatic trimming of high-mannose modification by mannosidase, which can be inhibited by kifunensine, resulting in blockade of global complex glycan modification²³. We found that Kifunensine treatment indeed abolished the smear bands above 55kDa of wild-type SIGIRR (**Fig. 2D**), indicating that the smear band represents the complex glycan modified SIGIRR.

SIGIRR^{ΔE8} is a common variant in colon cancer cells with reduced complex glycan modification. To determine whether the defect in SIGIRR glycosylation was due to changes of glycosylation enzymes (*trans*-defect) or alterations/mutations in SIGIRR (*cis*-defect), we transfected exogenous SIGIRR cDNA into the VACO400 cells that showed defective SIGIRR glycosylation (**Fig. 1A**). Surprisingly, the exogenous SIGIRR was normally modified by complex glycan, suggesting a *cis*-defect of endogenous SIGIRR (**Fig. 3A**). We then performed 5' rapid amplification of cDNA ends (5'RACE) to analyze of RNA from Vaco400 cells and repeatedly encountered two SIGIRR transcripts: a full-length SIGIRR mRNA and a novel variant that lacks the exon8 (SIGIRR^{ΔE8}) (**Fig. 3B**). The exon8 encodes part of the intracellular TIR domain. Exclusion of the exon8 does not lead to frameshift of the 3' sequence, resulting in a SIGIRR isoform with a shorter cytoplasmic tail. The percentage of isoform (SIGIRR^{ΔE8}) over total SIGIRR was increased in the colorectal cancer specimen as well as the colon cancer cell lines compared to freshly isolated normal human colonic epithelial cells (**Fig. 3C and Supple. Fig. 1A-B**). We tested the ability of SIGIRR^{ΔE8} to inhibit IL-1R signaling with luciferase assay. Deletion of exon8 substantially abolished the ability of SIGIRR to inhibit IL-1β induced NFκB activation (**Fig. 3D**). Interestingly, SIGIRR^{ΔE8} exhibited substantial loss of smear band above 55kDa compared to the full-length SIGIRR although the missing exon does not contain the motifs for N-linked glycosylation (**Fig. 3D**). While kifunensine treatment shrank the size of full-length SIGIRR, it failed to reduce the size of SIGIRR^{ΔE8}, implying lack of complex glycan modification on SIGIRR^{ΔE8} (**Fig. 3E**).

RNA sequencing reveals increased expression of SIGIRR^{ΔE8} in colorectal cancer. To more rigorously assess the association of SIGIRR^{ΔE8} with human colon cancer, we analyzed RNA sequencing data of 68 pairs of normal and cancerous colorectal tissue samples¹⁸. To quantify SIGIRR^{ΔE8} levels, we took two different approaches to analyze the RNA sequencing data: calculating both the junction reads and computing the number of reads from exon 8. We first compared the number of junction reads of exon7-9 (exclusion of exon8) with that of exon8-9 (inclusion of exon8). We calculated the ratio of exon7-9 (exclusion of exon8) reads to exon8-9 (inclusion of exon8) reads for each sample to compute the percentage of SIGIRR^{ΔE8} as part of the total SIGIRR transcript in cancer and paired normal tissue. The analysis detected a statistically significant increase of the junction reads for the exclusion of exon8 (SIGIRR^{ΔE8}) in the colorectal cancer (**Fig. 4A**). In a second approach, we normalized the abundance of exon8 to a reference exon (exon3) by computing the ratio of RPKM (Reads Per Kilobase per Million mapped reads) values (RPKM^{Exon8}/RPKM^{Exon3}). Indeed, we found that tumor samples had reduced RPKM^{Exon8}/RPKM^{Exon3} compared with the normal tissue (**Fig. 4B**) and this reduction is held regardless of the choice of reference exon (**Supple. Fig.2**). It should be noted that, although SIGIRR^{ΔE8} showed increased expression in the cancer samples, it is not exclusively expressed by only cancer cells as SIGIRR^{ΔE8} accounts for 10% of the total SIGIRR transcripts in normal tissue (**Fig. 4A-B**). Recent studies have suggested that normal intestinal stem cells express a gene signature similar to that of the colorectal cancer stem cells. We therefore examined whether the level of SIGIRR^{ΔE8} is elevated in the LGR5+ cells in both normal and cancer. We analyzed the relative abundance of SIGIRR^{ΔE8} in LGR5+ and LGR5- cells sorted from human colon but failed to detect a difference in SIGIRR^{ΔE8}. The results suggest that the detected increase of the percentage of SIGIRR^{ΔE8} over total SIGIRR expression in colon cancer tissues might be due to the oncogenic transformation rather than reflecting the cellular constituent of the samples (**Supple. Fig 3A**). Moreover, we did not detect difference in the percentage of SIGIRR^{ΔE8} over total SIGIRR expression in normal colon organoids maintained in stem cell culture (high LGR5 expression) and differentiation culture conditions (low LGR5 expression) (**Supple. Fig 3B**). Taken together, these data indicate that tumor tissues express significantly more SIGIRR^{ΔE8} compared with paired normal tissues, suggesting that the exclusion of exon8 is an event associated with colorectal cancer.

We then wondered whether there might be differential gene expression profiles between SIGIRR^{ΔE8} high versus SIGIRR^{ΔE8} low colon cancers. We interrogated the RNA sequencing dataset and found that more than 100 genes were significantly up-regulated in SIGIRR^{ΔE8} high cancer tissue comparing with that in SIGIRR^{ΔE8} low cancer tissue (**Supple. Table 1**). Among the most significantly up-regulated genes, we found increased expression of immune-response associated genes (such as T cell receptor alpha, immunoglobulin heavy variable and defensins), implying the possible association of SIGIRR^{ΔE8} high colon cancer with a pro-inflammatory microenvironment (**Fig. 4C**). This feature is consistent with the role of SIGIRR as a negative regulator of inflammatory responses. In addition, we also found up-regulation of genes implicated in cancer growth (aldehyde dehydrogenase 1, Dual oxidase 2, Cathepsin E) and metastasis (Matrix metalloproteinase 8,10 and 20) in SIGIRR^{ΔE8} high cancer tissue comparing with that in SIGIRR^{ΔE8} low cancer tissue (**Fig. 4C**).

SIGIRR^{ΔE8} is a dominant negative mutant retained in the ER and traps full-length SIGIRR. It is important to note that both 5' RACE and RNA sequencing analyses detected substantial expression of full-length SIGIRR transcript in colon cancer cell lines (**Fig. 3C**) and colon cancer tissues (**Fig. 4B-C**). One critical question is whether and how SIGIRR^{ΔE8} exerts its impact in the presence of full-length SIGIRR. Since SIGIRR could form homodimer through its ectodomain and TIR domain^{11 13}, we postulated that the SIGIRR^{ΔE8} might act in a dominant negative fashion via its interaction with full-length SIGIRR. We indeed found that SIGIRR^{ΔE8} attenuated the ability of full-length SIGIRR to inhibit IL-1R signaling in a dose dependent manner (**Fig. 5A**). SIGIRR^{ΔE8} also blocked the complex glycan

modification of SIGIRR and converted it to the high-mannose modified SIGIRR (band below 55kDa) (**Fig. 5A**). These data are consistent with a dominant negative role of SIGIRR^{ΔE8}. In support of this, we indeed found that SIGIRR could interact with SIGIRR^{ΔE8} (**Fig. 5B**). Notably, the high-mannose modified SIGIRR bands from co-transfection of wild-type SIGIRR and SIGIRR^{ΔE8} resembled the endogenous SIGIRR band pattern in the Vaco400 cell line, implicating the possible dominant negative role of endogenous SIGIRR^{ΔE8} in suppressing the complex glycan modification full-length SIGIRR in the Vaco400 cell line (**Supple. Fig. 1C**).

Since our data showed that SIGIRR^{ΔE8} blocks the complex glycan modification of full-length SIGIRR, we wondered whether SIGIRR^{ΔE8} might have a defect in cell surface expression and also interferes with that of full-length SIGIRR. Thus, we first employed *in situ* protein biotinylation assay to specifically quantify the expression of SIGIRR on the cell membrane. While the complex glycan modified full-length SIGIRR (when expressed alone) was found on the cell membrane, we failed to detect the expression of SIGIRR^{ΔE8} on cell membrane (**Fig. 5C**). However, the co-expression of SIGIRR^{ΔE8} prevented the cell surface expression of full-length SIGIRR (**Fig. 5C**). The colon cancer cell line Ls174t expresses endogenous full-length SIGIRR and SIGIRR^{ΔE8} (**Fig 3C**. SIGIRR^{ΔE8} makes up 45% of total SIGIRR). We also detected complex glycan modified endogenous SIGIRR on the cell surface (**Fig.5D**). Interestingly, SIGIRR was reported to be an interacting partner with RPN1 in a large-scale two-yeast hybrid screening²⁴. RPN1 is a subunit of the ER resident oligosaccharyltransferase complex²⁵, implicated in facilitating N-linked glycosylation for a subset of membrane proteins. We indeed detected interaction of SIGIRR with RPN1 (**Fig. 5D**). Notably, it is the SIGIRR without complex glycan modification that binds to RPN1 and SIGIRR^{ΔE8} showed much stronger interaction with RPN1 compared to full-length SIGIRR(**Fig. 5E**). Interestingly, co-expression with SIGIRR^{ΔE8} enhanced the interaction between full-length SIGIRR with RPN1 (**Fig. 5E**), suggesting that SIGIRR^{ΔE8} might inhibited the function of full-length SIGIRR by trapping it in the ER and preventing the decoration by complex glycan.

Considering the loss of cell surface expression of SIGIRR^{ΔE8} and its ability to trap full-length SIGIRR, we wondered whether the increased expression of SIGIRR^{ΔE8} might lead to abnormal SIGIRR subcellular localization in human colon cancer tissue. We stained for SIGIRR in human colonic normal and cancer tissue. A stark difference in the localization of SIGIRR was observed between normal and cancer tissues (**Fig. 5F**), including sporadic colorectal cancer and colitis associated cancer tissues. Normal colonic epithelial cells showed predominantly membrane localization of SIGIRR, as indicated by co-localization with membrane marker Na⁺-K⁺ ATPase (**Fig. 5F**). The membrane localization of SIGIRR is maintained throughout the crypt, including the bottom of the crypt where the stem cells reside (**Supple. Fig 3C-D**). In contrast, colorectal cancer cells exhibited cytoplasmic staining of SIGIRR and increased co-localization with the ER marker RPN1 (**Fig. 5F**), implicating increased retention of SIGIRR in the ER in human colon cancer.

To characterize the pattern of SIGIRR expression in a larger cohort, we stained for SIGIRR in a total of 110 cases of colorectal cancer and normal samples on a tissue array. Consistently, while SIGIRR was localized to the cell membrane in normal tissue and adenoma tissue, its cytoplasmic expression was increased in the cancer tissues (**Supple. Fig. 4**). We observed an inverse correlation between the membrane expression of SIGIRR (as measured by the co-localization signal with Na⁺-K⁺ ATPase) and the tumor grade, with the poorly differentiated cancer (Grade III) showing predominantly cytoplasmic SIGIRR staining (**Supple. Fig. 5A**). In support of this, while the percentage of SIGIRR^{ΔE8} is significantly elevated in the cancer tissues compared to normal and adenoma tissues tissues (**Supple. Fig 5C**), which is suggestive of a cancer-specific event.

Loss of modification by complex glycan is sufficient to inactivate SIGIRR *in vivo*. Our results above suggest that the mode of action that inactivates SIGIRR in colorectal cancer represents a novel mechanism whereby functionality of SIGIRR is abolished through its altered subcellular localization and glycosylation. We next seek to establish transgenic models of SIGIRR mutants to test the importance of complex glycan modification and cell surface expression of SIGIRR *in vivo*. Since SIGIRR^{ΔE8} also lacks the critical TIR domain essential for the molecule to function (interacting with TLRs-IL-1R family members), SIGIRR^{ΔE8} may not be ideal for testing the impact of loss of complex glycan modification and reduced cell surface expression of SIGIRR. Interestingly, SIGIRR^{N86/102S} (with point mutations at N86 and N102 to serines) had substantially reduced complex glycan modification and failed to come to cell surface (**Fig. 2A and 6A**), similar to defect observed with SIGIRR^{ΔE8}, making it an ideal candidate for testing our hypothesis. Furthermore, SIGIRR^{N86/102S} was indeed defective of inhibiting IL-1R signaling in cell culture experiments (**Fig. 6B**). Thus, we decided to use SIGIRR^{N86/102S} to study the role of complex glycan modification and cell surface expression of SIGIRR in tumorigenesis.

We created gut-epithelial-specific SIGIRR-transgenic mice by expressing flag-tagged wild-type SIGIRR (WT-SIGIRR) and SIGIRR^{N85/101S} (MT-SIGIRR) under the control of transcriptional regulatory elements derived from a fatty acid-binding protein gene²⁶. The glycosylation sites are conserved between mouse and human SIGIRR, with human N86 and N102 corresponding to mouse N85 and N101 (**Fig. 2B**). The SIGIRR transgenes were specifically expressed in intestine and colon but not in other tissues¹² (data not shown). SIGIRR^{N85/101S} showed loss of the smear bands above 55kDa (**Fig. 6C**), indicating that mutation at these two sites reduced the complex glycan modification *in vivo*. Immunofluorescence revealed that MT-SIGIRR exhibited predominantly cytoplasmic localization whereas WT-SIGIRR showed strong cell surface expression (**Fig. 6D**).

To compare the functionality of MT-SIGIRR with WT-SIGIRR *in vivo*, we crossed WT-SIGIRR and MT-SIGIRR transgenic mice onto SIGIRR^{-/-} background and subjected them to AOM-DSS treatment. As we reported before¹², re-expression of WT-SIGIRR in colonic epithelial cells reduced the number and size of tumors (**Supple. Fig.6**). In contrast, mice with MT-SIGIRR had similar tumor burden in comparison with SIGIRR^{-/-} mice (**Supple. Fig.6**). Taken together, the results suggest that loss of complex glycan modification and cell surface expression renders SIGIRR defective of suppressing colitis-associated tumorigenesis.

Since co-expression of SIGIRR^{N85/101S} suppressed the full-length SIGIRR modification and cell surface expression *in vitro* (**Fig. 6A**), we then tested the dominant negative function of the MT-SIGIRR *in vivo*. We crossed MT-SIGIRR onto SIGIRR^{+/-} background to test the impact of MT-SIGIRR expression on endogenous SIGIRR protein. Consistent with the *in vitro* experiments, MT-SIGIRR expression significantly reduced the modification of endogenous wild-type SIGIRR protein in the mouse colonic epithelial cells (**Fig. 7A**). Moreover, expression of the MT-SIGIRR increased the average tumor number and tumor size when the mice were subjected to AOM-DSS treatment (**Fig. 7B and 7C**). Interestingly, the phenotype of MT-SIGIRR is reminiscent of the gene expression profile observed in SIGIRR^{ΔE8} high human colon cancers, which is suggestive of an inflammatory microenvironment. Among the genes that are upregulated in SIGIRR^{ΔE8} high human colon cancer, we found increased expression of Mmp8 and Duox2 in the tumors from MT-SIGIRR, SIGIRR^{+/-} mice compared to that of the SIGIRR^{+/-} mice (**Fig. 7D**). In addition, MT-SIGIRR expressing tumors showed increased expression of inflammatory cytokines such as IL-17A and IL-6. Consistent with the cytokine levels, activation of downstream transcription factors STAT3^{27 28 29} and NFκB^{30 31}, both of which are tumor-promoting factors, was increased in the tumors expressing MT-SIGIRR. Increased activation of these transcription factors was associated with elevated expression their target genes including *Bcl-xL* and *Cox2* (31,39) (**Fig. 7E**). The results suggest that MT-SIGIRR is capable of acting as dominant negative

mutant to suppress wild-type SIGIRR function in vivo, leading to inflamed microenvironment that favors tumor formation and growth.

Consistent with the increased tumor growth in the MT-SIGIRR, SIGIRR^{+/-} mice, we found that overexpression of SIGIRR^{ΔE8} and SIGIRR^{N86/102S} in HT-29 colon cancer cell line increased the colony formation capacity of the HT-29 cells in the presence of IL-1β compared to those with empty vector (**Fig 7F**). Taken together, our data suggest that modification by complex glycan and cell surface expression is required for SIGIRR to inhibit excessive intestinal inflammation and tumorigenesis.

Discussion

In this study, we identified a dominant negative isoform of SIGIRR, SIGIRR^{ΔE8} that is strongly associated with human colon cancer. Increased expression of SIGIRR^{ΔE8} was found in a cohort of 68 cases of colorectal cancer tissues compared with paired normal tissues. SIGIRR^{ΔE8} exhibited reduced modification by complex glycan with increased retention in the cytoplasm. This cytoplasmic retention of SIGIRR^{ΔE8} is likely due to its interaction with ER protein RPN1, resulting in decreased expression on the cell membrane and loss of the inhibitory effect on IL-1R signaling. On the other hand, SIGIRR^{ΔE8} retains the ability to interact with full-length SIGIRR thereby exerting a dominant negative effect on the function of full-length SIGIRR. Importantly, SIGIRR^{ΔE8} exhibited drastically increased cytoplasmic localization and decreased cell surface expression in human colon cancer compared to normal tissue, consistent with the increased ratio of SIGIRR^{ΔE8} versus full-length SIGIRR. Thus the exclusion of exon8 is a mode of action commonly taken by colorectal cancer to inactivate SIGIRR via dominant negative effect of SIGIRR^{ΔE8} (**Supple. Fig. 7**).

The tumorigenesis of CRC is a multistep process, during which mutations on oncogenes and tumor suppressor genes accumulate to enable malignant transformation^{2,3}. Alternative splicing is one of the mechanisms cancer cells use to overcome suppression to gain growth advantage³². Our previous structure-function analysis has shown that the TIR domain of SIGIRR contributes to the suppression of TLR4, IL-1R and ST2¹³. Exclusion of the exon 8 compromises the integrity of the TIR domain in SIGIRR. Meanwhile, deletion of exon 8 also prevented the protein to traffic to the cell membrane. Thus, exclusion of exon 8 represents an efficient way to ensure the inactivation of SIGIRR to gain growth advantage.

One important question is what controls the expression of SIGIRR^{ΔE8}. Interestingly, sequence analysis predicted exon 8 as a “weak” exon (with a high probability of exclusion) due to the short intron between exon 7 and exon 8 and a secondary structure within this intron. Intriguingly, we found a CTCF binding site in exon 8; and CTCF binding to its cognate DNA motif has been reported to promote the inclusion of weak exons (36). Notably, the binding of CTCF can be reduced by methylation on its binding site. As such, we postulate that in the normal colonic epithelial cells, CTCF constitutively binds to the cognate sequence in exon8 to promote the expression of full length SIGIRR. However, the CTCF binding may be reduced as a result of the hyper-methylation in the cancer cells, leading to expression of SIGIRR^{ΔE8}. Our preliminary results indeed showed that the expression of SIGIRR^{ΔE8} was decreased by treatment with decitabine (unpublished data), an inhibitor for DNA methyltransferase. The regulation of SIGIRR^{ΔE8} expression by methylation and CTCF represents an interesting prospect for future investigation.

Increased ER retention of SIGIRR^{ΔE8} was an unexpected observation. However the regulation of protein trafficking by *cis*-elements was documented before. A likely possibility is that, the deletion of

exon 8 changes the conformation of the cytoplasmic domain of SIGIRR, which in turn exposed a cryptic ER retention signal that promotes the retrograde transport of the protein from Golgi. In fact, there is a putative arginine based ER retention signal³³ (334-337 LRGR) in the C-terminus of SIGIRR, which is preserved in the SIGIRR^{ΔE8}. Therefore, the regulation of SIGIRR modification by complex glycan and its membrane expression may be tightly regulated by retrograde transport, as abnormal retrograde trafficking has been linked to many diseases³². Recently, a study found that dysregulation of the trafficking of TLRs leads to spontaneous intestinal inflammation. Collectively, the drastic impact of exclusion of exon 8 on the intracellular trafficking and glycosylation of SIGIRR may represent a novel mode of action that promotes cancer development.

Exclusion of exon 8 resulted in aberrant trafficking of SIGIRR, which leads to a drastic loss of complex glycan modification and abolishes its cell surface expression. Colon cancer cells are known to exhibit abnormal glycosylation of proteins^{34, 35}. We used a glycosylation mutant that showed substantially reduced complex glycan modification and defective cell surface expression to model the impact of SIGIRR^{ΔE8} in tumorigenesis. By re-expressing wild-type and glycosylation mutant SIGIRR specifically in the colonic epithelia cells of SIGIRR-deficient mice, we demonstrated that the complex glycan modification and cell surface expression is required for the functionality of SIGIRR *in vivo*. Future studies are required to investigate whether SIGIRR might be inactivated in a subset of colon cancer patients at the levels of glycosylation without impacting on its intracellular trafficking.

Figure Legends

Figure 1. SIGIRR loses modification in colon cancer. **A.** Lysates of normal epithelial cells isolated from human colon epithelium (normal colonic epithelial cells) and colon cancer cell lines (VACO cell lines) were analyzed by western blot. **B.** Lysates of normal epithelial cells isolated from normal human colon epithelium (Normal 1-10) and colorectal cancer tissue (Cancer1-5) were analyzed by western blot.

Figure 2. SIGIRR is N-linked glycosylated protein. **A.** 3 μ g of FLAG tagged wild-type and mutant SIGIRR cDNAs were transfected into HeLa cells and harvested for western blot analysis. **B.** Partial cDNA sequences of human and mouse SIGIRR showing the conserved N-linked glycosylation motifs (underlined). Asterisks indicate conserved amino acid residues. **C.** Normal colon epithelial cell lysates from 3 individuals were treated(+) or untreated(-) with PNGase F to remove N-linked glycosylation. Treated lysates were subjected to western blot. **D.** 3 μ g of FLAG tagged wild-type SIGIRR cDNA was transfected into HeLa cells followed by treatment with kifunensine at 5ng/mL for indicated time and western blot.

Figure 3. SIGIRR ^{Δ E8} is a common variant in colon cancer cells with reduced complex glycan modification. **A.** VACO 400 cells were transfected with FLAG-tagged SIGIRR(+) or empty vector followed by western blot. **B.** RNA from Vaco400 cells was used for 5' RACE analysis using primer targeting 5' end (RACE P) and oligo-dT targeting polyA tail. The product from the reaction was resolved on a 1.5% agarose gel. **C.** Quantitative analysis of the of SIGIRR ^{Δ E8} versus full-length SIGIRR transcript expressed as percentage of the SIGIRR ^{Δ E8} in normal colonic epithelial cells, colorectal cancer tissue and colon cancer cell lines. Locations of amplicons used in the assay are indicated in B (A1 and A2) **D.** Indicated amounts of full-length SIGIRR or SIGIRR ^{Δ E8} were transfected into HeLa cells together with NF κ B dependent luciferase followed by luciferase assay and western blot. **E.** 3 μ g of full-length SIGIRR or SIGIRR ^{Δ E8} cDNA was transfected into HeLa cells. 8 hours after transfection, cells were treated with 5ng/mL kifunensine for indicated time and harvested for western blot analysis. Error bar represents standard error of mean (S.E.M.) of 3 technical replicates.

Figure 4. RNA sequencing reveals increased expression of SIGIRR ^{Δ E8} in colorectal cancer. RNA sequencing data of 68 pairs of normal colon and colorectal cancer was analyzed for reads distribution. **A.** Each dot represents the percentage of SIGIRR ^{Δ E8} as a part of total SIGIRR transcript, calculated based the ration of junction read number (exon7-9 vs exon7-8). **B.** Each dot represents the $\text{Log}_2(\text{RPKM}^{\text{Exon8}}/\text{RPKM}^{\text{Exon 3}})$ value of each sample, which was derived by calculating the ratio of RPKM values of exon8 and the exon3, followed by transforming the data with Log function with 2 as base. Line and error bars represent means and 95% confidence interval. **C.** Volcano plot showing the log_2 (fold difference) and $-\text{log}_{10}$ (P values) of genes up-regulated in SIGIRR ^{Δ E8} high tumors compared to SIGIRR ^{Δ E8} low tumors. Genes of functional interest are highlighted in red and listed in the table on the right.

Figure 5. SIGIRR ^{Δ E8} is a dominant negative mutant and prevents the cell surface expression and complex glycan modification of full-length SIGIRR. **A.** Indicated amount of HA tagged full-length SIGIRR and FLAG tagged SIGIRR ^{Δ E8} were transfected into HeLa cells together with NF κ B dependent luciferase. Transfected cells were subjected luciferase assay and western blot analysis. Error bar represents S.E.M. of 3 technical replicates. **B.** HeLa cells were transfected with either 2 μ g HA tagged full-length SIGIRR alone or together with 4 μ g of FLAG tagged SIGIRR ^{Δ E8}. Transfected cells were lysed and lysates were immunoprecipitated with anti-FLAG antibody followed by western

blot. **C.** HeLa cells were transfected with indicated amounts full-length SIGIRR and/or SIGIRR^{ΔE8}. Transfected cells were subjected to *in situ* biotinylation assay followed by western blot analysis. **D.** Cancer cell line Ls174t with expression of endogenous SIGIRR (SIGIRR^{ΔE8} makes up 45% of total SIGIRR, Fig 3C.) with stable expression of scramble shRNA or shRNA targeting endogenous SIGIRR were subjected to *in situ* biotinylation assay(left) or immunoprecipitation(right) with anti-RPN1 antibody followed by western blot. **E.** HeLa cells were co-transfected with 2ug FLAG-tagged RPN1 and a total of 4ug HA tagged full-length SIGIRR and/or HA tagged SIGIRR^{ΔE8}. Transfected cells were lysed and the lysates were immunoprecipitated with anti-FLAG antibody followed by western blot analysis. **F.** Paraffin embedded sporadic colorectal cancer, colitis associated cancer tissue and their respective paired normal control were stained with anti-SIGIRR and anti-Na⁺-K⁺ ATPase (membrane marker, left) or anti-RPN1(ER marker, right) primary antibodies followed by corresponding secondary antibodies and DAPI. The staining was visualized using confocal microscopy under 40X (Scale bar= 50μm) or 62X (Scale bar= 3μm) magnification. All experiments were repeated at least 3 times yielding consistent results. Ctr: IgG control, IP: immunoprecipitation; PD: pull-down; WCL: whole cell lysates.

Figure 6. Loss of modification by complex glycan is sufficient to inactivate SIGIRR. **A.** HeLa cells were transfected with SIGIRR, SIGIRR^{ΔE8} or SIGIRR^{N86/106S} and subjected to *in situ* biotinylation assay followed by western blot analysis. PD: pull-down; WCL: whole cell lysates. **B.** HeLa cells were transfected with indicated amount with indicated amount of SIGIRR (WT), or SIGIRR^{N86/106S} (N86/10S) together with NFκB dependent luciferase followed by luciferase assay and western blot. Error bar represents S.E.M. of 3 technical replicates. **C.** Colon lysates from mice of indicated genotypes were subjected to western blot analysis. **D.** Colon tissue from mice of indicated genotypes were stained with FLAG antibody to visualize the localization of the transgene product.

Figure 7. Loss of modification by complex glycan is sufficient to inactivate SIGIRR in tumorigenesis. **A.** Colonic epithelial cell lysates from MT-SIGIRR, SIGIRR^{+/-} mouse and SIGIRR^{+/-} mouse was subjected to western blot analysis with anti-SIGIRR antibody. **B.** Mouse of indicated genotypes were subjected to AOM-DSS treatment. Tumor numbers and sizes were recorded and plotted. (N=7 for SIGIRR^{+/-}, N=10 for MT-SIGIRR, SIGIRR^{+/-}) **C.** Representative macroscopic view of colons from mice of indicated genotypes after the AOM-DSS treatment and H&E staining of tumors. **D.** Tumors from mice of indicated genotypes were subjected to real-time PCR analysis of indicated genes. **E.** Tumor lysates were subjected to western blot. Each lane represents one mouse. **E.** HT-29 cells were infected with lentivirus carrying an empty vector, shRNA targeting SIGIRR, or SIGIRR^{ΔE8} cDNA under a CMV promoter. The cells were cultured in the presence or absence of IL-1β for 5 days followed by crystal violet stain for formed colonies and colometric quantification of the colony formation. Error bar represents S.E.M * indicates p<0.05.

References:

1. **Siegel R**, Ward E, Brawley O, et al. Cancer statistics, 2011: the impact of eliminating socioeconomic and racial disparities on premature cancer deaths. *CA Cancer J Clin* 2011;61:212-36.
2. **Fearon ER**, Vogelstein B. A genetic model for colorectal tumorigenesis. *Cell* 1990;61:759-67.
3. **Markowitz SD**, Bertagnolli MM. Molecular origins of cancer: Molecular basis of colorectal cancer. *N Engl J Med* 2009;361:2449-60.
4. **Fukata M**, Shang L, Santaolalla R, et al. Constitutive activation of epithelial TLR4 augments inflammatory responses to mucosal injury and drives colitis-associated tumorigenesis. *Inflamm Bowel Dis* 2011;17:1464-73.
5. **Santaolalla R**, Sussman DA, Ruiz JR, et al. TLR4 activates the beta-catenin pathway to cause intestinal neoplasia. *PLoS One* 2013;8:e63298.
6. **Ullman TA**, Itzkowitz SH. Intestinal inflammation and cancer. *Gastroenterology* 2011;140:1807-16.
7. **Kaler P**, Augenlicht L, Klampfer L. Macrophage-derived IL-1beta stimulates Wnt signaling and growth of colon cancer cells: a crosstalk interrupted by vitamin D3. *Oncogene* 2009;28:3892-902.
8. **Zhao J**, Zepp J, Bulek K, et al. SIGIRR, a negative regulator of colon tumorigenesis. *Drug Discov Today Dis Mech* 2011;8:e63-e69.
9. **Garlanda C**, Riva F, Bonavita E, et al. Decoys and Regulatory "Receptors" of the IL-1/Toll-Like Receptor Superfamily. *Front Immunol* 2013;4:180.
10. **Thomassen E**, Renshaw BR, Sims JE. Identification and characterization of SIGIRR, a molecule representing a novel subtype of the IL-1R superfamily. *Cytokine* 1999;11:389-99.
11. **Wald D**, Qin J, Zhao Z, et al. SIGIRR, a negative regulator of Toll-like receptor-interleukin 1 receptor signaling. *Nat Immunol* 2003;4:920-7.
12. **Xiao H**, **Gulen MF**, Qin J, et al. The Toll-interleukin-1 receptor member SIGIRR regulates colonic epithelial homeostasis, inflammation, and tumorigenesis. *Immunity* 2007;26:461-75.
13. **Qin J**, Qian Y, Yao J, et al. SIGIRR inhibits interleukin-1 receptor- and toll-like receptor 4-mediated signaling through different mechanisms. *J Biol Chem* 2005;280:25233-41.
14. **Garlanda C**, Riva F, Polentarutti N, et al. Intestinal inflammation in mice deficient in Tir8, an inhibitory member of the IL-1 receptor family. *Proc Natl Acad Sci U S A* 2004;101:3522-6.
15. **Garlanda C**, Riva F, Veliz T, et al. Increased susceptibility to colitis-associated cancer of mice lacking TIR8, an inhibitory member of the interleukin-1 receptor family. *Cancer Res* 2007;67:6017-21.
16. **Xiao H**, Yin W, Khan MA, et al. Loss of single immunoglobulin interleukin-1 receptor-related molecule leads to enhanced colonic polyposis in Apc(min) mice. *Gastroenterology* 2010;139:574-85.
17. **Kelleher DJ**, Kreibich G, Gilmore R. Oligosaccharyltransferase activity is associated with a protein complex composed of ribophorins I and II and a 48 kd protein. *Cell* 1992;69:55-65.
18. **Seshagiri S**, **Stawiski EW**, **Durinck S**, et al. Recurrent R-spondin fusions in colon cancer. *Nature* 2012;488:660-4.
19. **Dobin A**, Davis CA, Schlesinger F, et al. STAR: ultrafast universal RNA-seq aligner. *Bioinformatics* 2013;29:15-21.
20. **Grady WM**, Myeroff LL, Swinler SE, et al. Mutational inactivation of transforming growth factor beta receptor type II in microsatellite stable colon cancers. *Cancer Res* 1999;59:320-4.
21. **Willson JK**, Bittner GN, Oberley TD, et al. Cell culture of human colon adenomas and carcinomas. *Cancer Res* 1987;47:2704-13.
22. **Johnson JL**, Jones MB, Ryan SO, et al. The regulatory power of glycans and their binding partners in immunity. *Trends Immunol* 2013;34:290-8.
23. **Ryan SO**, Bonomo JA, Zhao F, et al. MHCII glycosylation modulates *Bacteroides fragilis* carbohydrate antigen presentation. *J Exp Med* 2011;208:1041-53.
24. **Stelzl U**, Worm U, Lalowski M, et al. A human protein-protein interaction network: a resource for annotating the proteome. *Cell* 2005;122:957-68.
25. **Wilson CM**, Roebuck Q, High S. Ribophorin I regulates substrate delivery to the oligosaccharyltransferase core. *Proc Natl Acad Sci U S A* 2008;105:9534-9.
26. **Saam JR**, Gordon JI. Inducible gene knockouts in the small intestinal and colonic epithelium. *J Biol Chem* 1999;274:38071-82.

27. **Bollrath J**, Phesse TJ, von Burstin VA, et al. gp130-mediated Stat3 activation in enterocytes regulates cell survival and cell-cycle progression during colitis-associated tumorigenesis. *Cancer Cell* 2009;15:91-102.
28. **Grivnikov S**, Karin E, Terzic J, et al. IL-6 and Stat3 are required for survival of intestinal epithelial cells and development of colitis-associated cancer. *Cancer Cell* 2009;15:103-13.
29. **Putoczki TL**, Thiem S, Loving A, et al. Interleukin-11 is the dominant IL-6 family cytokine during gastrointestinal tumorigenesis and can be targeted therapeutically. *Cancer Cell* 2013;24:257-71.
30. **Greten FR**, Eckmann L, Greten TF, et al. IKKbeta links inflammation and tumorigenesis in a mouse model of colitis-associated cancer. *Cell* 2004;118:285-96.
31. **Karin M**, Greten FR. NF-kappaB: linking inflammation and immunity to cancer development and progression. *Nat Rev Immunol* 2005;5:749-59.
32. **Adler AS**, McClelland ML, Yee S, et al. An integrative analysis of colon cancer identifies an essential function for PRPF6 in tumor growth. *Genes Dev* 2014;28:1068-84.
33. **Michelsen K**, Yuan H, Schwappach B. Hide and run. Arginine-based endoplasmic-reticulum-sorting motifs in the assembly of heteromultimeric membrane proteins. *EMBO Rep* 2005;6:717-22.
34. **Christiansen MN**, Chik J, Lee L, et al. Cell surface protein glycosylation in cancer. *Proteomics* 2014;14:525-46.
35. **Kim YS**, Ahn YH, Song KJ, et al. Overexpression and beta-1,6-N-acetylglucosaminylation-initiated aberrant glycosylation of TIMP-1: a "double whammy" strategy in colon cancer progression. *J Biol Chem* 2012;287:32467-78.
36. **Shukla S**, Kavak E, Gregory M, Imashimizu M, Shutinoski B, Kashlev M, Oberdoerffer P, Sandberg R, Oberdoerffer S. CTCF-promoted RNA polymerase II pausing links DNA methylation to splicing. *Nature*. 2011 Nov 3;479(7371):74-9

Author names in bold designate shared co-first authorship

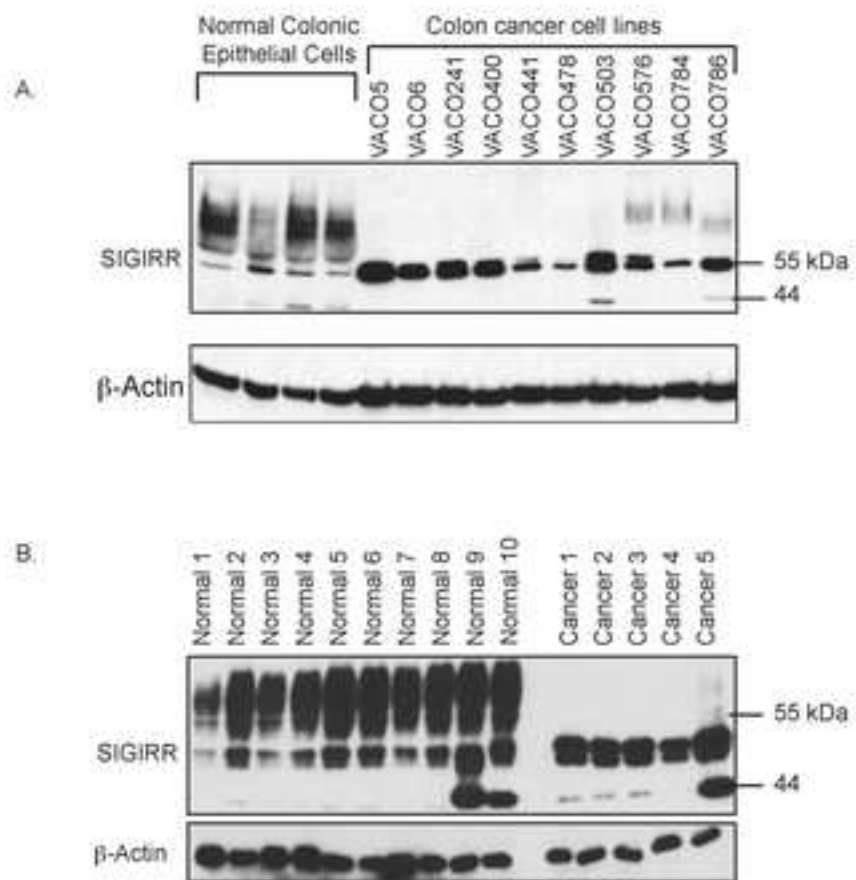


Figure 1

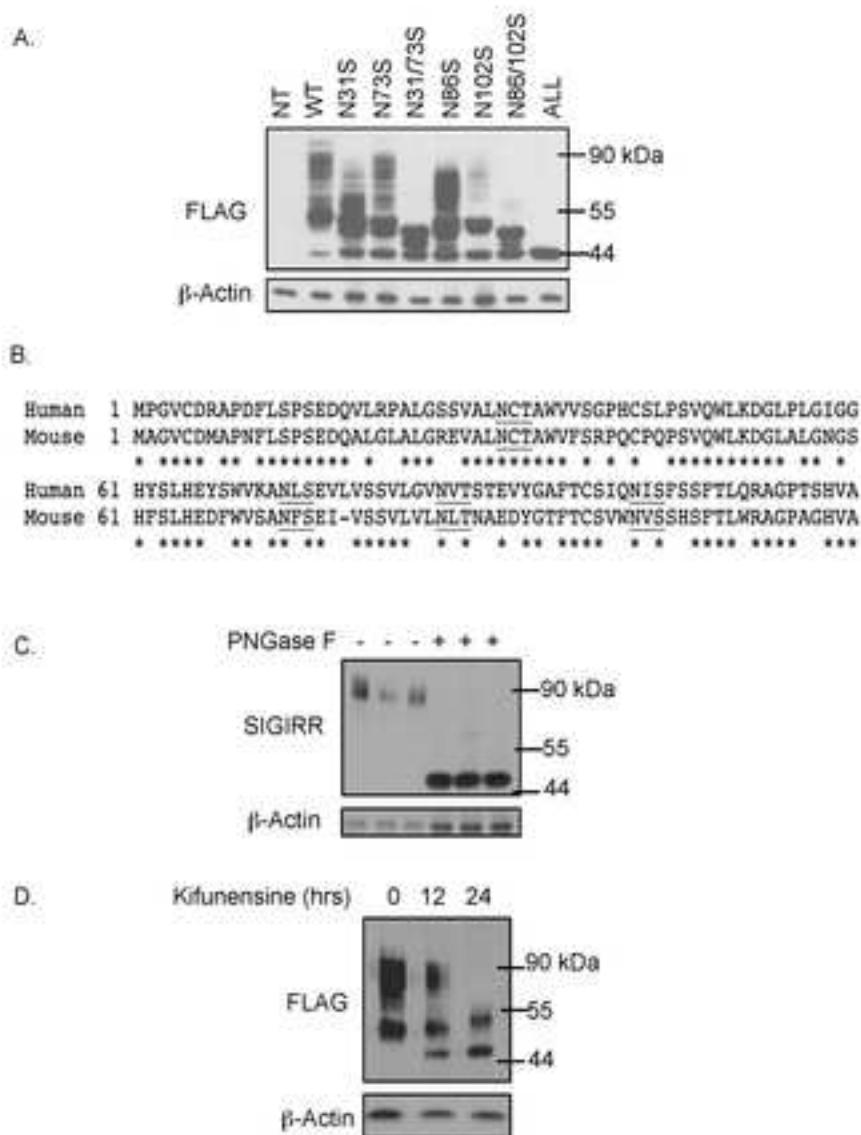


Figure 2

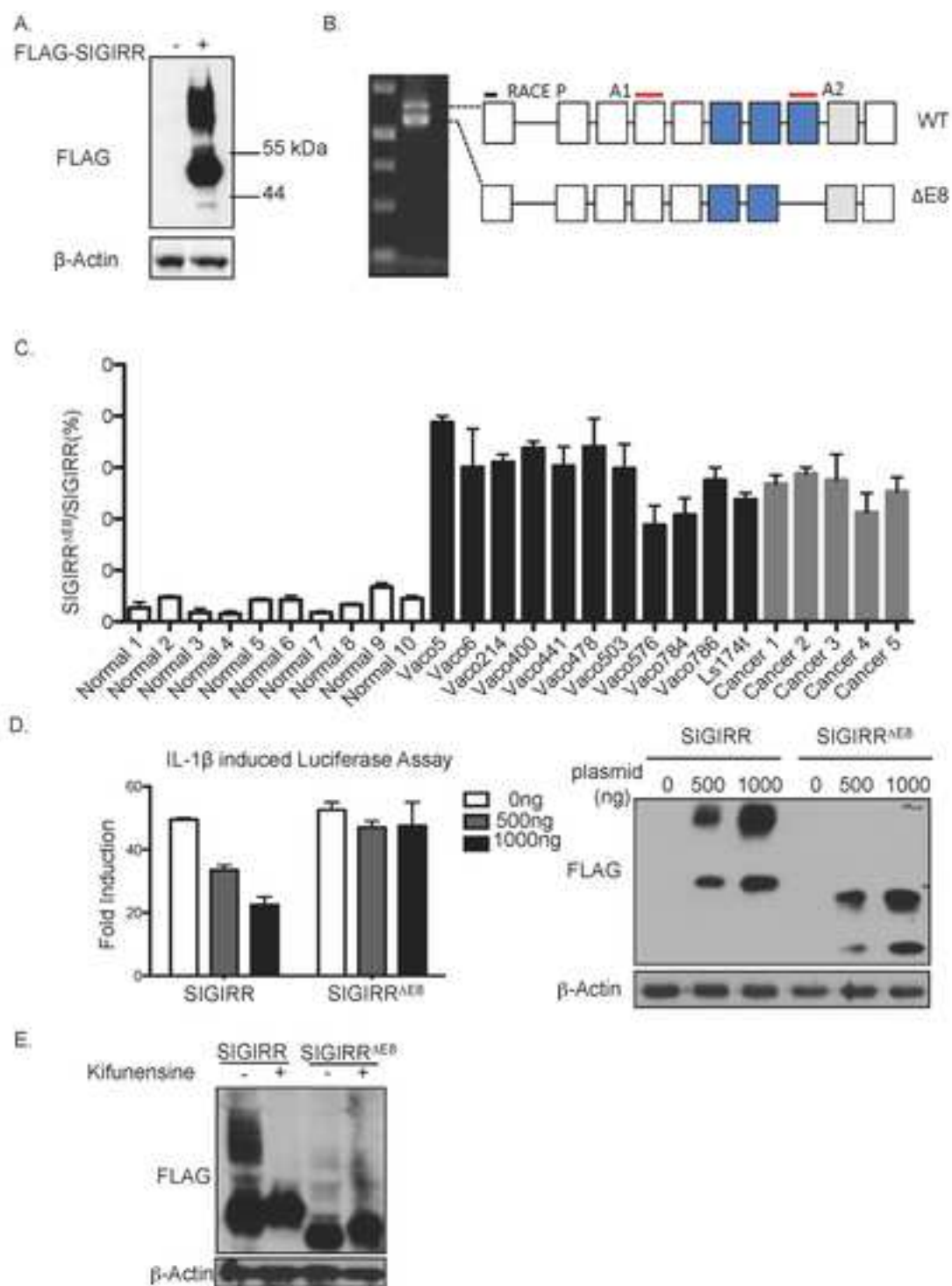


Figure 3

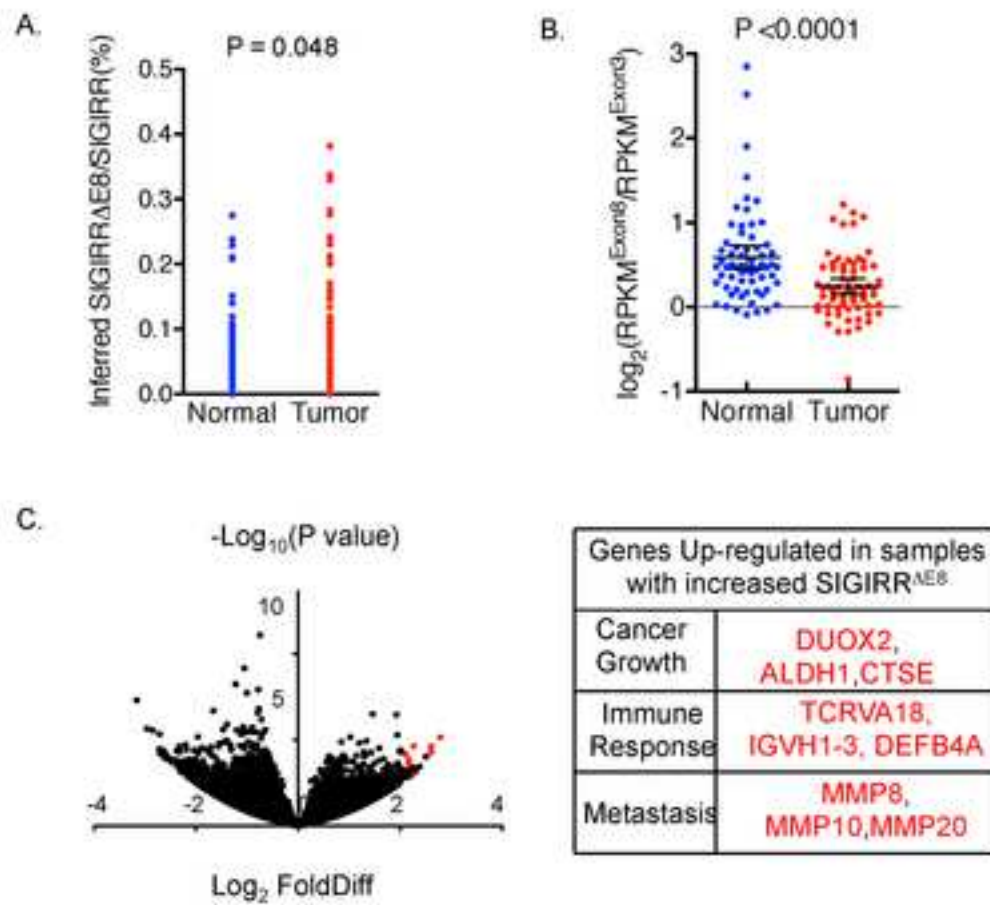


Figure 4.

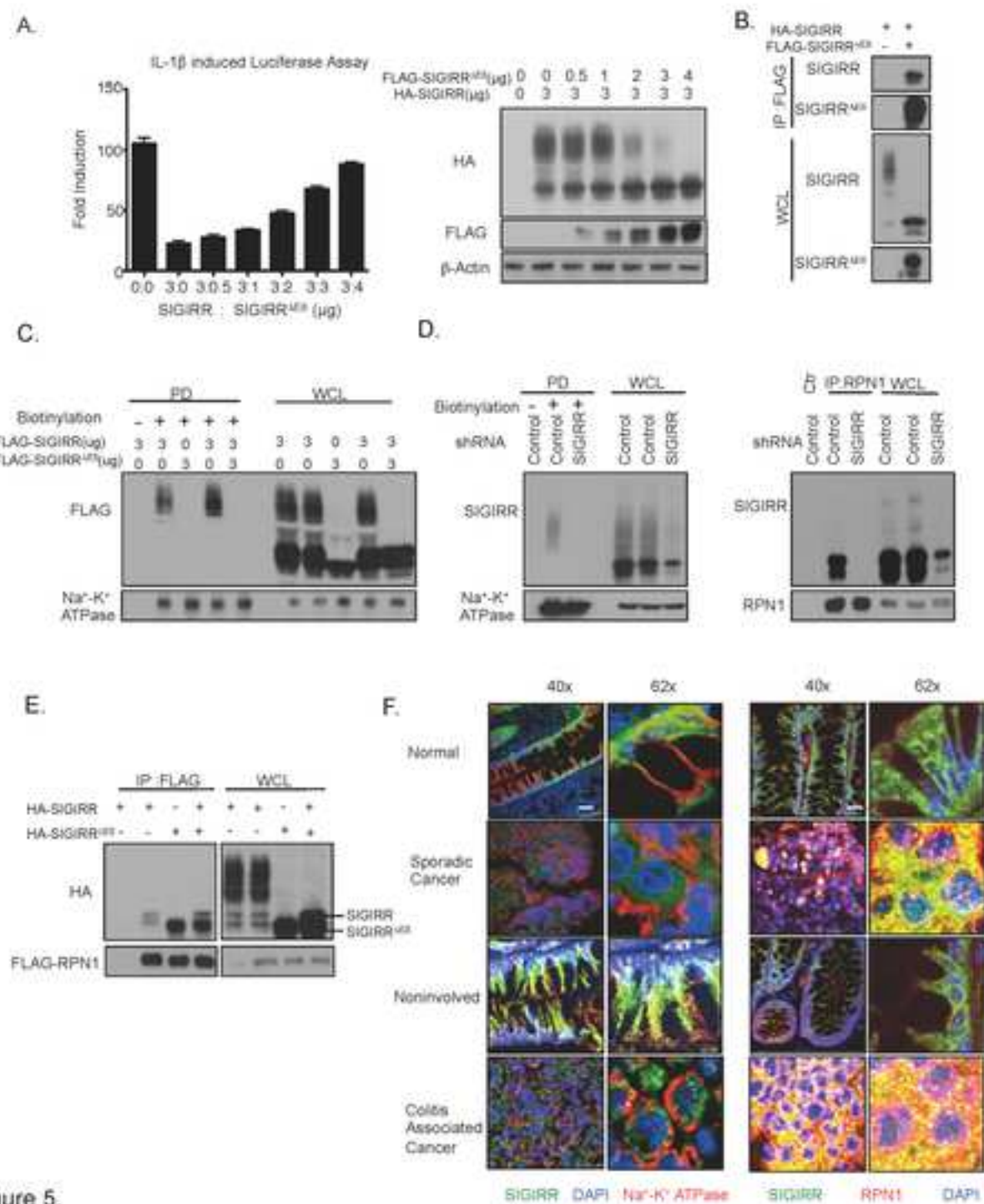


Figure 5.

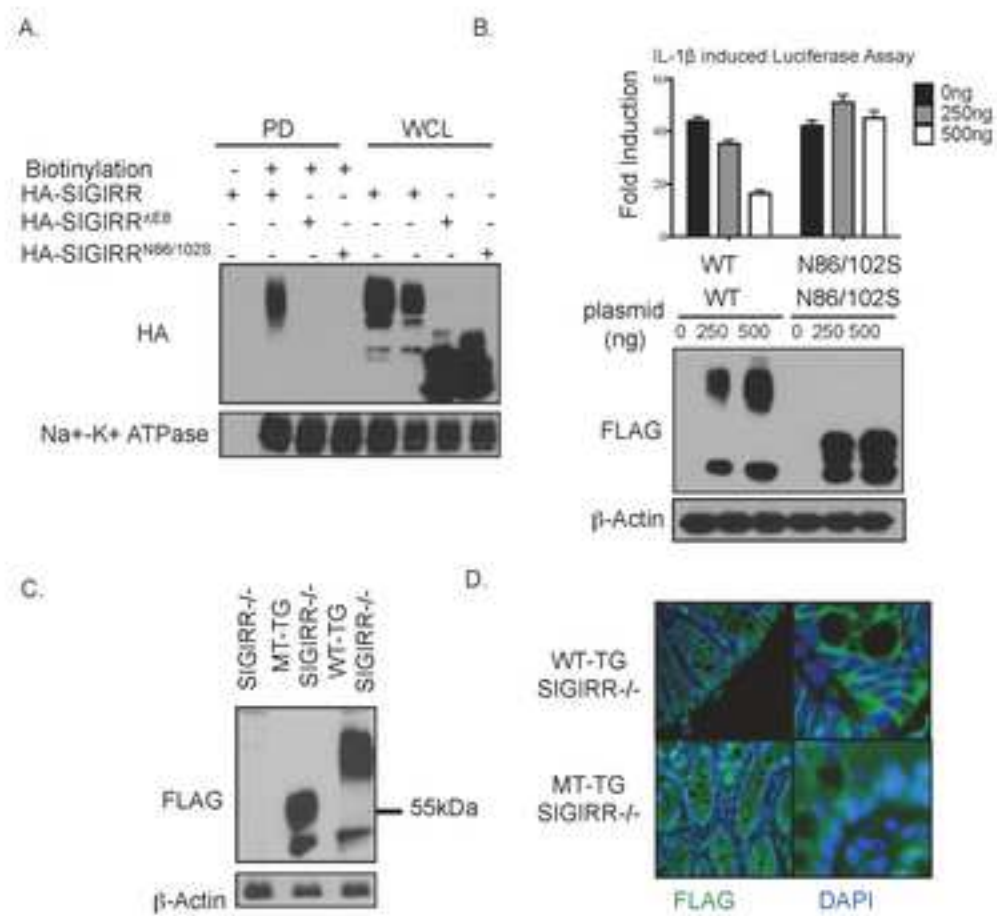


Figure 6.

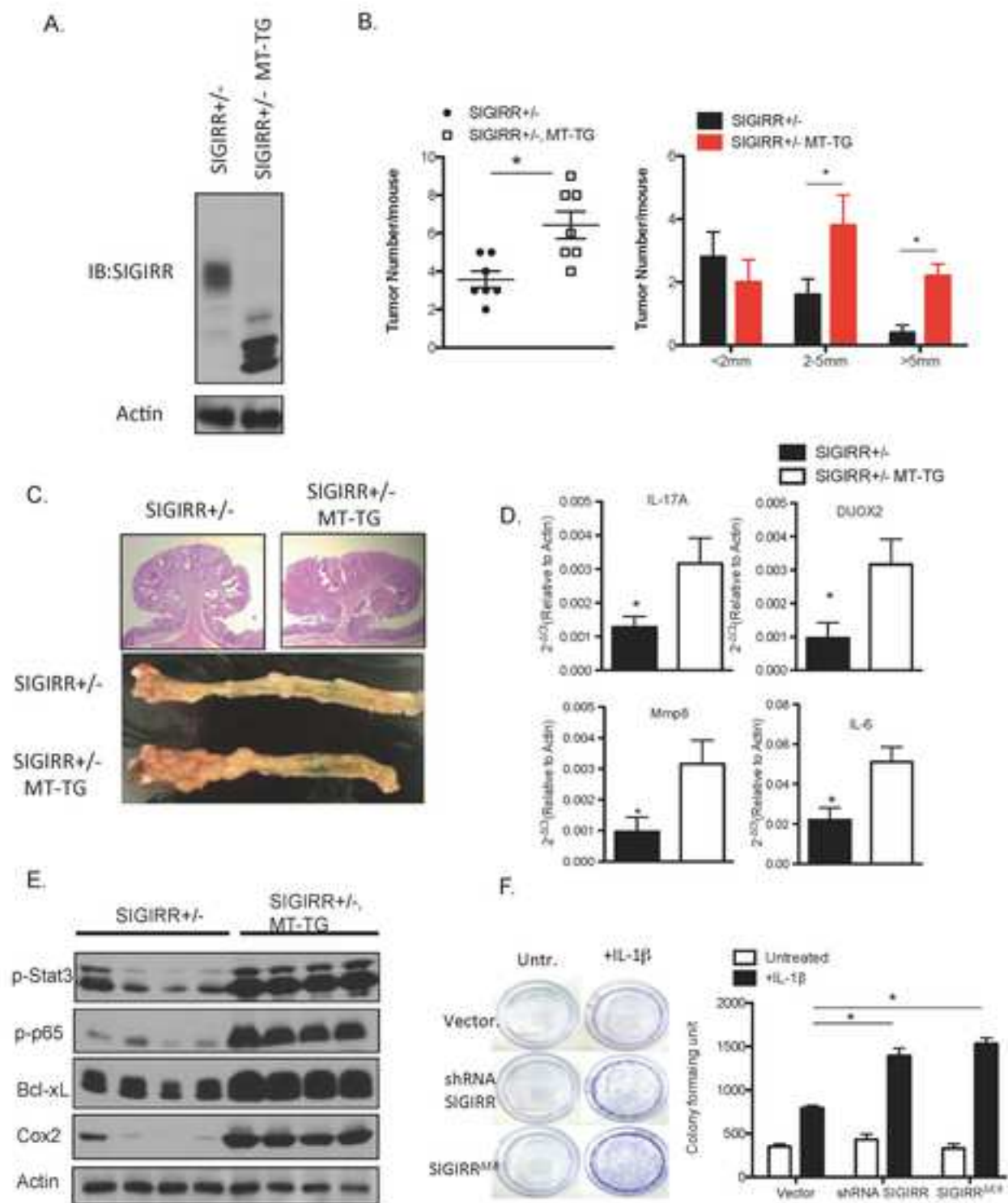


Figure 7.

Supplemental Material and Methods

Luciferase reporter assays HeLa cells were transiently transfected using FuGENE 6 (Roche Diagnostics) with NF κ B luciferase reporter plasmid following the manufacturer's protocol. Empty vector was used to ensure all wells received equal amounts of DNA. 24 h after transfection, cells were stimulated with 1ng/mL IL-1 β for 8 hours. Cells were lysed and luciferase activity was assessed using Reporter lysis buffer and Luciferase Assay Reagent (Promega). All results reported are technical triplicates representing at least three independent experiments.

Plasmid DNA encoding N-terminal FLAG-tagged SIGIRR was cloned into the vector pCDAN3.1 (+) purchased from Invitrogen. Site-directed mutagenesis was performed on N-terminal FLAG-tagged SIGIRR on pcDNA3.1(+) using QuickChange kit from Agilent Technologies according to the manufacturer's instruction. In all cases, the asparagine was mutated to serine on the plasmid. 5'RACE was performed using a kit from Invitrogen (18374-058) according to the manufacturer's instruction. HA and FLAG-tagged Full-length SIGIRR and SIGIRR Δ E8 expression plasmids were constructed by subcloning from the 5'RACE product into a pcDNA3.1(+) vector.

Construction of SIGIRR-Transgenic Mouse Transgenic construct was generated as described before. DNA encoding mouse SIGIRR was placed under the control of transcriptional regulatory elements derived from a fatty acid-binding protein gene followed by the human growth hormone reporter gene (hGH). A Flag tag was included at the N terminus of SIGIRR to distinguish the transgene from the endogenous gene. Site-directed mutagenesis was performed on the construct carrying wildtype SIGIRR sequence to generate mutant transgene. Both constructs were sent to the Transgenic and Targeting Facility at Case Western Reserve University. Mice carrying transgenes were genotyped with polymerase chain reaction to detect presence of hGH sequence. Transgenes were bred with SIGIRR knockout mice to generate SIGIRR $^{-/-}$, WT-SIGIRR and SIGIRR $^{-/-}$, MT-SIGIRR strains.

Tumorigenesis Procedure 8-week-old mice (SIGIRR $^{-/-}$, Fabp1-SIGIRR/Fabp1-SIGIRR^{N85/101S} and their SIGIRR $^{-/-}$ littermates were on mixed C57BL/6 \times 129/SvJ background) were injected with AOM (Sigma) dissolved in 0.9% NaCl intraperitoneally at a dose of 12.5 mg/kg body weight. 5 days after injection, mice were treated with 2.5% DSS in drinking water, then followed by regular water for 16 days. This cycle was repeated twice. 2 weeks after the last DSS treatment, mice were sacrificed and murine colon was removed and flushed carefully with PBS buffer. Colon tumors were counted and measured under a stereomicroscope. Representative tumors were paraffin embedded and sectioned at 5 μ m. Histology analysis was carried out on H&E-stained tumor sections.

In situ Biotinylation, Immunoprecipitation Biotinylation was performed by rinsing transfected cells with cold PBS followed by incubation with freshly prepared 10mM sulfo-NHS-biotin dissolved in cold PBS for 2 hours. The labeling process was stopped by siphoning away the labeling reagent and quenching the with 100mM glycine dissolved in PBS. The cells were then harvested and lysed for lysates. The supernatant was collected for western blot or ELISA analysis. Co-immunoprecipitation was performed by incubating cell lysates with antibodies and protein A beads, or avidin conjugated beads at 4 $^{\circ}$ C overnight. Precipitated protein-beads complex was washed with lysis buffer followed by elution with 2X SDS-PAGE loading buffer.

Transfection, kifunensine, PNGase F treatment and western blot. Transfection was performed using Fugene 6 according to the manufacturer's protocol. For kifunensine treatment, the inhibitor was added 8 hours after transfection and the cells were harvested 48 hours after

transfection. PNGase F was purchased from New England Biolabs and used according to the manufacturer's instruction. Cells were lysed in lysis buffer (0.5% Triton X-100, 20 mM HEPES (pH 7.4), 150 mM NaCl, 12.5 mM β -glycerophosphate, 1.5 mM $MgCl_2$, 10 mM NaF, 2 mM dithiothreitol (DTT), 1 mM sodium orthovanadate, 2 mM EGTA, 1 mM phenylmethylsulfonyl fluoride and complete protease inhibitor cocktail from Roche). Western blots were performed after the SDS-PAGE following standard procedure. For analysis of immunoprecipitation samples, anti-light chain secondary antibody (Jackson Immuno Research) was used.

Quantitative real-time PCR In all experiments, RNA was extracted with TRIZol (Invitrogen) followed by reverse transcription with SuperScript II Reverse Transcriptase (Life Technologies) according to the manufacturer's instruction. Real-time PCR analysis was performed use SYBR Green master mixes (Agilent Technologies). Primer sequences are as follow: Mmp8 forward -5' CCAGCACCTATTCACCTACCTC 3' reverse-5' AGCATCAAATCTCAGGTGGG3' ; Duox2 forward-5' CTTCCACATCTACTTCCTGGTC 3' reverse-5' AATGTCTTGGGTCTCTGGAAC 3'; SIGIRR exon4 forward -5' ACTACAGCCTCCACGAGTAC 3' reverse-5' CCATAGACTTCAGTGCTGGTC 3' ; SIGIRR exon8 forward -5' CTCTTGGTGAACCTGAGCC 3' reverse-5' CCCTCGAAGGTGATGAAGATG 3'. The standard curve for quantification of SIGIRR^{ΔE8} was established by amplifying cDNA of full-length SIGIRR and SIGIRR^{ΔE8} mixed at indicated ratio (**Supple. Fig 1A** total input 10ng plasmids) and calculating the Ct difference.

Immunofluorescence Formalin-fixed and paraffin-embedded colon sections or tumor samples were deparaffined, rehydrated, and pretreated with 3% hydrogen peroxidase in PBS buffer for 20 minutes. Antigen retrieval in DAKO's antigen retrieval buffer was conducted in a steam cooker for 20 minutes at 96°C, followed by slowly cooling down at room temperature. After blocking with 10% normal goat serum, sections were incubated with primary antibody overnight at 4°C. Then, the sections are washed with PBST and stained with corresponding secondary antibodies and DAPI. The stained slides are subjected to confocal microscopy for analysis.

Colon culture Colon tissue from mice on the day 15 of the AOM-DSS protocol was washed in cold PBS supplemented with penicillin and streptomycin. The tissue was then cut into small pieces and cultured in 12-well flat bottom culture plates (Falcon) in serum-free RPMI medium supplemented with penicillin and streptomycin. After incubation at 37°C for 24 hr, medium was collected and subjected to ELISA using kit purchased from R&D. Colon organoids were isolated following previously described protocol. Briefly, the normal colon mucosa was isolated and minced. Minced tissue was subjected to collagenase I (Sigma) incubation for 30 minutes at 37 degree. Digested tissue was then filtered through a 70 μ m cell strainer and washed with DMEM/F12 medium. Isolated crypts were precipitated and embedded in matrigel and cultured in the presence of mouse wnt3a, human R-spondin1, human EGF and mouse Noggin (+WNR) or in the presence of human EGF only.

Cell sorting Normal human mucosa and cancer tissue was washed with cold PBS and minced. Minced tissue was then digested with collagenase I at 37 degree for 30 minutes. Isolated crypts were further digested with Trypsin LE (Life Technologies) for 10 minutes to create single cell suspension. Cells were then washed and stained with fluorophore conjugated antibodies. anti-human LGR5 antibody and anti-human EpCam antibody were purchased from Miltenyi Biotec .

Statistical Analysis Normality of data was not formally tested. Therefore non-parametric statistics was applied in all data analysis. Mann–Whitney U was used to determine the p value of mean difference in two-group comparison.

ACCEPTED MANUSCRIPT

Legends for Supplemental Figures and Table

Supplemental Figure 1. A. Standard curve for the quantification of the percentage of SIGIRR^{ΔE8} over total SIGIRR. **B.** Real-time PCR analysis of total SIGIRR expression in indicated samples using amplicon targeting the exon4. Error bar represents standard error of mean (S.E.M) of biological replicates. **C.** Increasing amounts of SIGIRR^{ΔE8} were co-transfected with full-length SIGIRR into HeLa cells. Cell lysates were subjected to western blot using anti-

SIGIRR antibody. Note the similar band pattern between co-expression of SIGIRR^{ΔE8} with full-length SIGIRR and the endogenous SIGIRR in Vaco400 cells.

Supplemental Figure 2. A. $\text{Log}_2(\text{RPKM}^{\text{Exon8}}/\text{RPKM}^{\text{Reference Exon}})$ values computed using RPKM values of other coding region exons as reference were plotted for each sample. **B.** $\text{Log}_2(\text{RPKM}^{\text{Exon8}}/\text{RPKM}^{\text{Reference Exon}})$ Values computed using RPKM values of other coding region exons as reference were plotted as bar graph showing the significant reduction in the tumor samples. * P value <0.01 **P value<0.001

Supplemental Figure 3. A. Normal colon mucosa and colorectal cancer tissue was enzymatically dissociated to generate single cell suspension. Cells were stained with FITC conjugated anti-Epcam and PE conjugated LGR5. Epcam+LGR5+ cells were sorted and subjected to real-time PCR analysis. **B.** Normal colon crypts were cultured under previously described condition to derive organoids. Established organoids were then cultured under stem cell condition (+WRN) or differentiating condition (-WRN) followed by real-time PCR analysis. **C.** Normal human colon paraffin section were stained with anti-SIGIRR (green), anti Na⁺-K⁺ATPase antibody (red) and DAPI. **D.** Normal human colon paraffin section were stained with anti-SIGIRR (green), anti β-Catenin antibody (red) and DAPI.

Supplemental Figure 4. Colon cancer tissue array of 110 cases was stained with anti-SIGIRR (green), anti-Na⁺-K⁺ATPase(red) antibodies and DAPI (blue). Representative images from normal colon tissues (**A**) and adenoma (**B**), grade I-II colorectal cancer tissues(**C and D**) and grade III colorectal cancer tissues (**E and F**) are shown. Scale bar= 25 μm

Supplemental Figure 5. A. Co-localization signal of SIGIRR and Na⁺-K⁺ATPase was quantified for each sample on the tissue array described in supplemental figure 4. The signal intensity was correlated with the tumor grade. **B.** Immunostaining of a stage II colon cancer for SIGIRR showing the progressive changes from normal to cancer. **C.** RNA from adenoma tissue (7 case in total) and normal tissue was analyzed with real-time PCR.

Supplemental Figure 6. Mice of indicated genotypes were subjected to AOM-DSS induced colon tumorigenesis. **A.** Tumor numbers were recorded and plotted. (N=8 for SIGIRR+/-, N=7 for SIGIRR-/-, N=15 for WT-SIGIRR, N=12 for MT-SIGIRR.) **B.** Tumor size distribution in mice underwent experiment described for A. **C.** Representative macroscopic view of colons from mice of indicated genotypes after the AOM-DSS treatment and H&E staining of tumors from mice of indicated genotypes. **D.** 15 days after the initiation of the tumorigenic protocol, the colons were taken for *ex vivo* culture for 12 hours. Supernatant from the organ culture were subjected to ELISA. (N=5, error bar represents S.E.M) **E.** Colons from experiments described for panel D were lysed and the lysates were subjected to western blot. Each lane represents one mouse. **F.** Gene expression analysis by real-time PCR of tumors from mice underwent AOM-DSS. Error bar represents S.E.M * indicates p<0.05, ** indicates p<0.0001

Supplemental Table 1 Top 100 up-regulated genes in SIGIRR^{ΔE8} high colorectal cancers

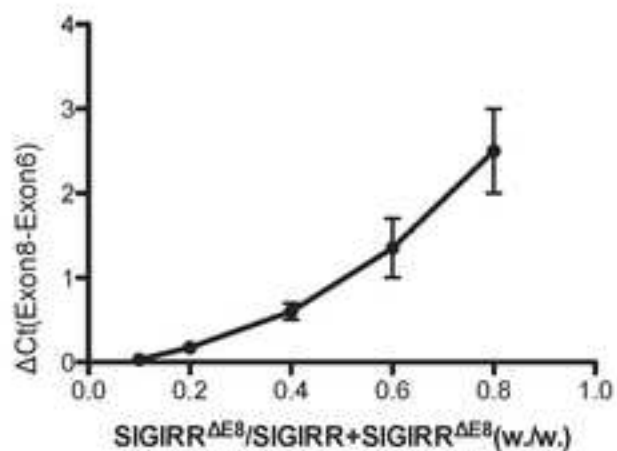
| Gene Description | Fold Change | Adjusted p value |
|---|-------------|------------------|
| Immunoglobulin heavy variable 1-3 | 10.79100639 | 1.25E-08 |
| Immunoglobulin heavy variable 1/OR15-3 | 6.885605208 | 7.03E-06 |
| Aldehyde dehydrogenase 1 family, member L1 | 6.084714683 | 2.41E-05 |
| Immunoglobulin kappa variable 6D-21 | 6.082007054 | 8.45E-05 |
| Cathepsin E | 6.068421107 | 5.08E-05 |
| RAD17 homolog | 5.671697711 | 2.86E-05 |
| Defensin, beta 4A | 5.661011918 | 9.59E-05 |
| Tripartite motif containing 72, E3 ubiquitin protein ligase | 5.193330706 | 0.00035181 |
| WAP four-disulfide core domain 12 | 4.940887474 | 0.00044488 |
| Family with sequence similarity 83, member C | 4.897490171 | 0.000705923 |
| Mucin 4, cell surface associated | 4.804269863 | 2.35E-05 |
| Membrane-spanning 4-domains, subfamily A, member 12 | 4.773043002 | 0.000770139 |
| Microsomal triglyceride transfer protein | 4.750526007 | 0.000393668 |
| Keratin 6B | 4.737665939 | 0.000953002 |
| Transient receptor potential cation channel, subfamily V | 4.565926869 | 0.000767522 |
| D-amino-acid oxidase [| 4.502168041 | 0.000577826 |
| Deleted in malignant brain tumors 1 | 4.499204033 | 0.001384927 |
| Transient receptor potential cation channel, subfamily V | 4.49755197 | 0.000704776 |
| SLC7A11 antisense RNA 1 | 4.496734603 | 0.000152557 |
| TMLHE antisense RNA 1 | 4.48738292 | 0.001209422 |
| Protease, serine, 1 (trypsin 1) | 4.486833221 | 0.001317118 |
| Cystatin S | 4.485949581 | 0.000244128 |
| MicroRNA 5587 | 4.463470593 | 0.001340198 |
| Myosin binding protein C, slow type | 4.450216641 | 0.001263645 |
| Matrix metalloproteinase 8 (neutrophil collagenase) | 4.421040045 | 0.001009067 |
| Neuropeptide Y receptor Y6 | 4.337598106 | 0.001181456 |
| Hydroxycarboxylic acid receptor 3 | 4.296538597 | 6.88E-05 |
| Immunoglobulin kappa joining 5 | 4.255872519 | 0.001498937 |
| Chloride channel accessory 4 | 4.229012122 | 0.001313344 |
| Immunoglobulin kappa variable 1D-27 | 4.185603042 | 0.001232669 |
| Cholinergic receptor, nicotinic, alpha 7 | 4.178820533 | 0.000571709 |
| V-set and immunoglobulin domain containing 2 | 4.127279852 | 0.001359981 |
| Dual oxidase 2 | 4.087002751 | 0.001836333 |
| Immunoglobulin heavy variable 6-1 | 4.063108143 | 0.000511038 |
| Phosphatase and actin regulator 2 pseudogene 1 [| 4.04135711 | 0.001686791 |
| Chymotrypsin-like elastase family, member 3B | 4.035446872 | 0.001626975 |
| Protease, serine, 33 | 4.034198651 | 0.001232605 |
| FERM and PDZ domain containing 3 | 4.02858679 | 0.001024602 |
| Xanthine dehydrogenase | 4.010987274 | 0.001104457 |
| Interleukin 13 receptor, alpha 2 | 4.002680226 | 4.42E-05 |
| T cell receptor alpha variable 18 | 3.998687428 | 0.000725179 |
| Matrix metalloproteinase 10 (stromelysin 2) | 3.992558873 | 0.001271347 |
| Immunoglobulin kappa variable 2-26 | 3.951600401 | 0.001279844 |
| Keratin 32 | 3.94905481 | 0.003522221 |

| | | |
|---|-------------|-------------|
| Solute carrier family 13 (sodium-dependent dicarboxylate transporter), member 2 | 3.9438296 | 0.003061587 |
| ATP-binding cassette, sub-family A (ABC1), member 12 | 3.935535025 | 0.001448535 |
| Nuclear receptor subfamily 1, group H, member 4 | 3.923146338 | 0.003684918 |
| Immunoglobulin kappa variable 1-16 | 3.909612378 | 0.002932452 |
| Immunoglobulin lambda variable 2-18 | 3.897372209 | 0.003857212 |
| Immunoglobulin heavy variable 3-48 | 3.895695358 | 0.001156257 |
| Hydroxycarboxylic acid receptor 2 | 3.881397594 | 0.00388553 |
| Immunoglobulin heavy variable 3-15 | 3.867017991 | 0.000457937 |
| Regenerating islet-derived 1 beta | 3.863446162 | 0.000914453 |
| Matrix metalloproteinase 20 | 3.844007957 | 0.000254919 |
| Proprotein convertase subtilisin/kexin type 1 | 3.841079319 | 5.30E-06 |
| Acyl-CoA oxidase-like | 3.834592062 | 0.004072552 |
| Keratin 37 | 3.830986264 | 0.002483995 |
| Transmembrane protease, serine 11E | 3.789640306 | 0.001257516 |
| Surfactant associated 2 | 3.787418565 | 3.46E-07 |
| Maestro heat-like repeat family member 2A | 3.768030838 | 0.001586669 |
| CD300 molecule-like family member d | 3.738782812 | 0.004875004 |
| Gliomedin | 3.738144225 | 0.004709175 |
| Solute carrier organic anion transporter family, member 4C1 | 3.698445541 | 0.004974919 |
| Glucosaminyl (N-acetyl) transferase 3, mucin type | 3.696547887 | 0.004475873 |
| Long intergenic non-protein coding RNA 1511 | 3.680602174 | 0.000427588 |
| Fructose-1,6-bisphosphatase 2 | 3.671008112 | 0.005737687 |
| POM121 transmembrane nucleoporin B (pseudogene) | 3.6694481 | 0.003659366 |
| V-set domain containing T cell activation inhibitor 1 | 3.665879761 | 0.003414012 |
| Hepatitis A virus cellular receptor 1 | 3.641632281 | 0.004996819 |
| ADP-ribosyltransferase 5 | 3.641173813 | 0.001865793 |
| Arachidonate 15-lipoxygenase | 3.636888903 | 0.005733402 |
| Immunoglobulin kappa variable 2D-24 | 3.634753674 | 0.002443329 |
| TAR DNA binding protein pseudogene 2 | 3.628337692 | 0.000589396 |
| Immunoglobulin lambda variable 2-23 | 3.62810549 | 0.006184943 |
| Immunoglobulin lambda constant 6 | 3.625289388 | 0.001810775 |
| Small proline-rich protein 2D | 3.614528068 | 0.004130302 |
| Transient receptor potential cation channel, subfamily A, member 1 | 3.611342872 | 0.006382652 |
| Hepsin | 3.589679497 | 0.000777594 |
| Pleckstrin homology domain containing, family G | 3.563481725 | 0.006934812 |
| Immunoglobulin lambda variable 6-57 | 3.560848072 | 0.002290553 |
| Keratin 6A | 3.560529202 | 0.005949099 |
| Insulin-like growth factor binding protein 1 | 3.554819224 | 0.003979318 |
| Carbonic anhydrase II | 3.554701171 | 0.004198011 |
| Mucin 5B, oligomeric mucus/gel-forming | 3.549785303 | 0.001247391 |
| Immunoglobulin heavy variable 3-23 | 3.539717146 | 0.007236282 |
| Solute carrier family 4 (sodium bicarbonate cotransporter), member 4 | 3.538834282 | 0.001099452 |
| Immunoglobulin heavy variable 3/OR16-6 | 3.530049121 | 0.002957845 |
| Mucin-like 1 | 3.525221616 | 0.000948065 |

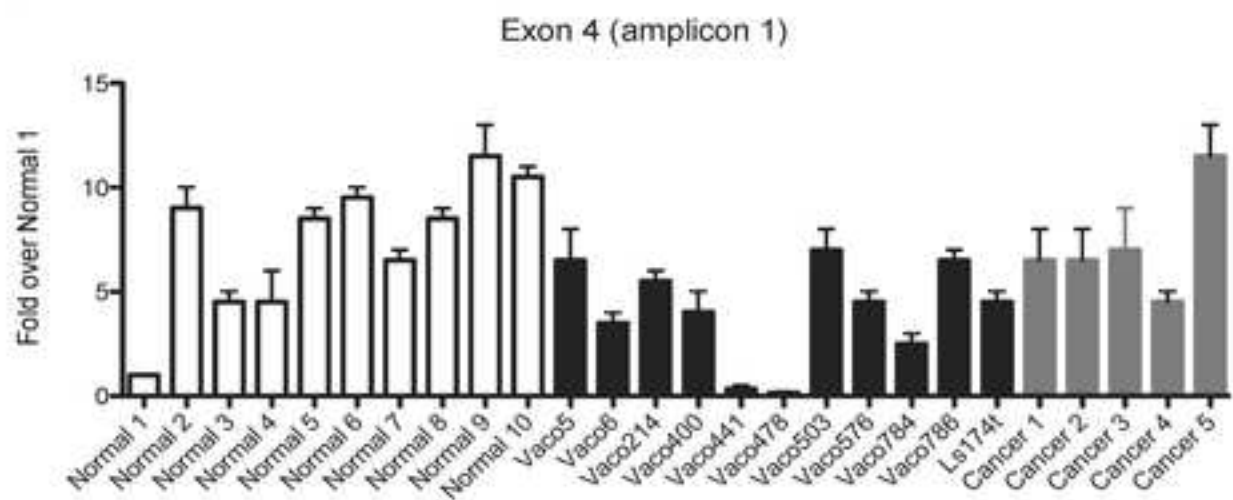
| | | |
|---|-------------|-------------|
| Immunoglobulin lambda variable 8-61 | 3.519610177 | 0.006039831 |
| Immunoglobulin kappa variable 1-27 | 3.516856642 | 0.005259029 |
| Keratin 3 | 3.51663443 | 0.005218816 |
| Sperm associated antigen 17 | 3.513435344 | 0.007608932 |
| EYA transcriptional coactivator and phosphatase 4 | 3.49913034 | 0.006622943 |
| Ubiquitin-conjugating enzyme E2 variant 2 | 3.485678047 | 0.000557363 |
| Dehydrogenase/reductase (SDR family) member 9 | 3.478656468 | 0.008038889 |
| Androgen-dependent TFPI-regulating protein | 3.472637185 | 0.007586122 |
| Butyrophilin-like 8 | 3.471366973 | 0.000919719 |
| Immunoglobulin heavy variable 2-5 | 3.446423183 | 0.008586999 |
| Immunoglobulin J polypeptide, linker protein | 3.442054932 | 0.008562378 |
| Protease, serine, 41 | 3.423634323 | 0.007638857 |

Supplemental Figure 1.

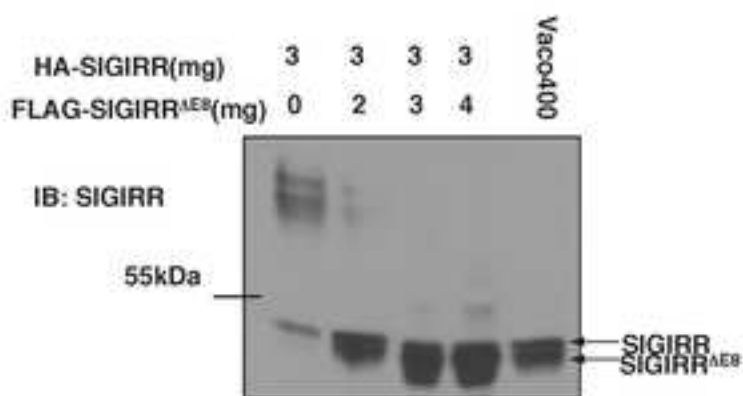
A.



B.

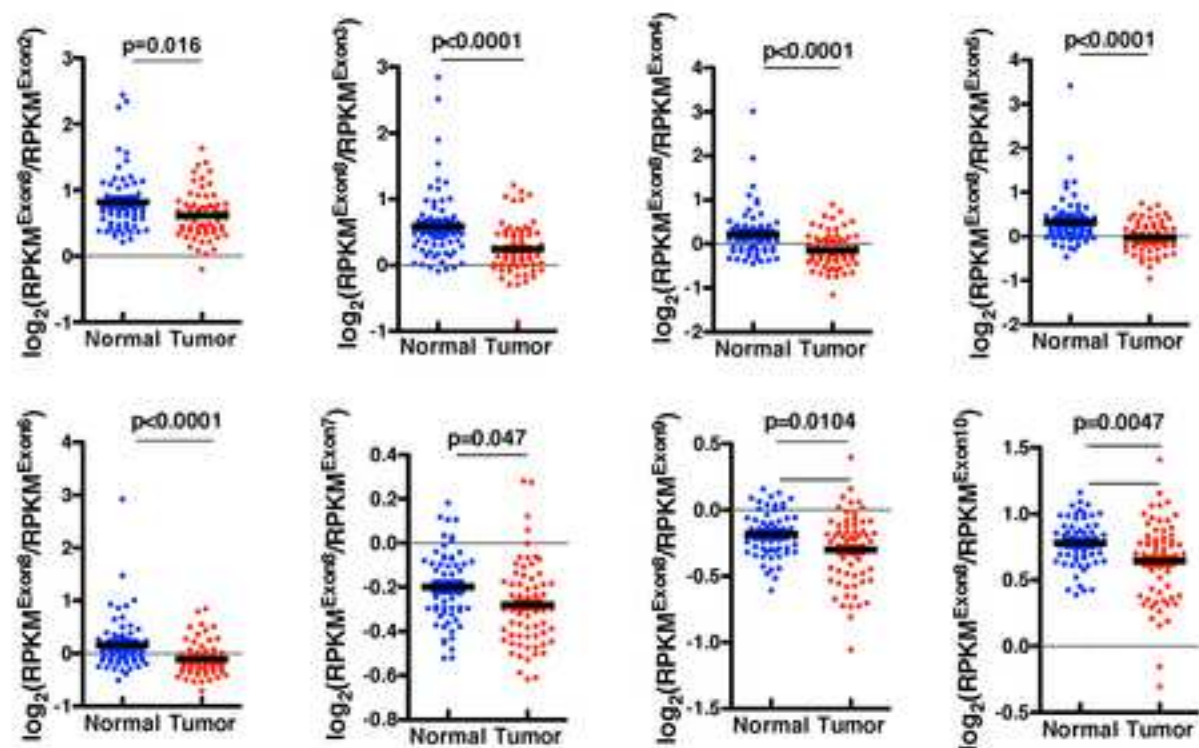


C.

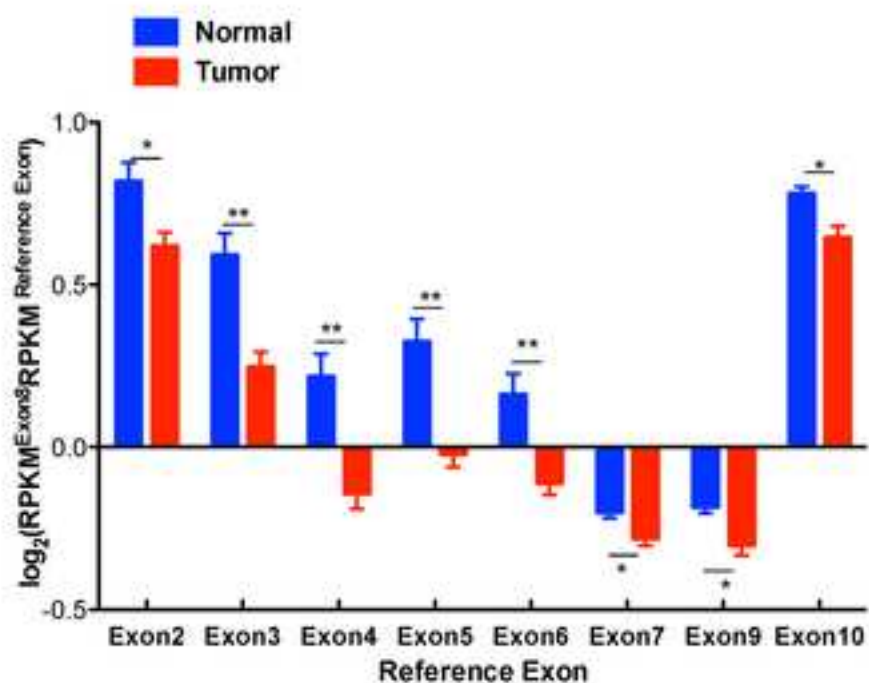


Supplemental Figure 2.

A.

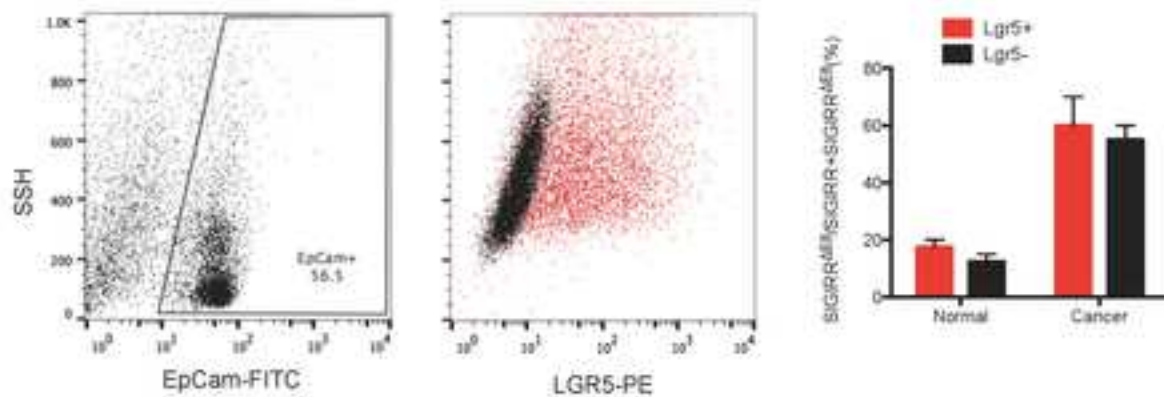


B.

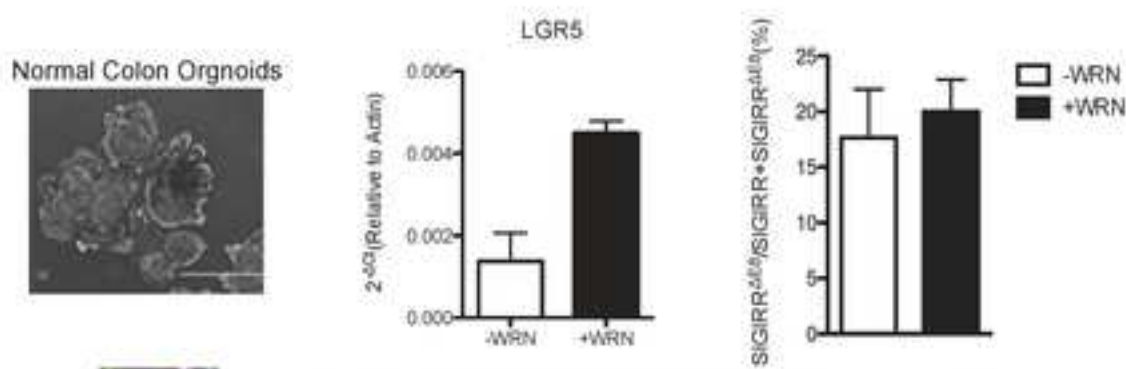


Supplemental Figure 3.

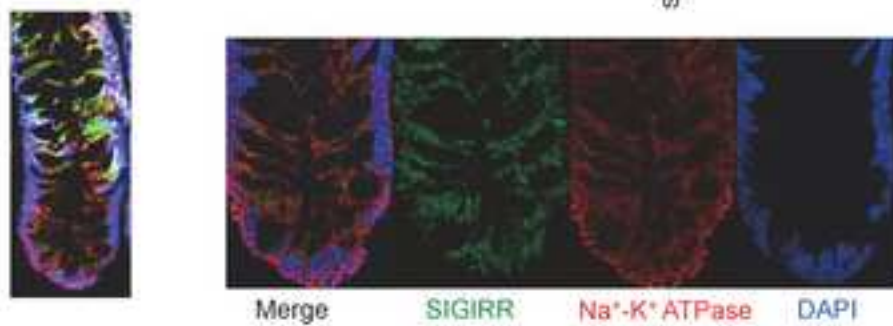
A.



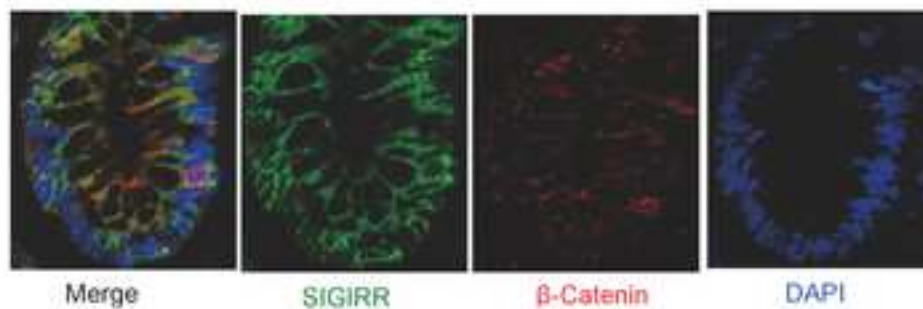
B.



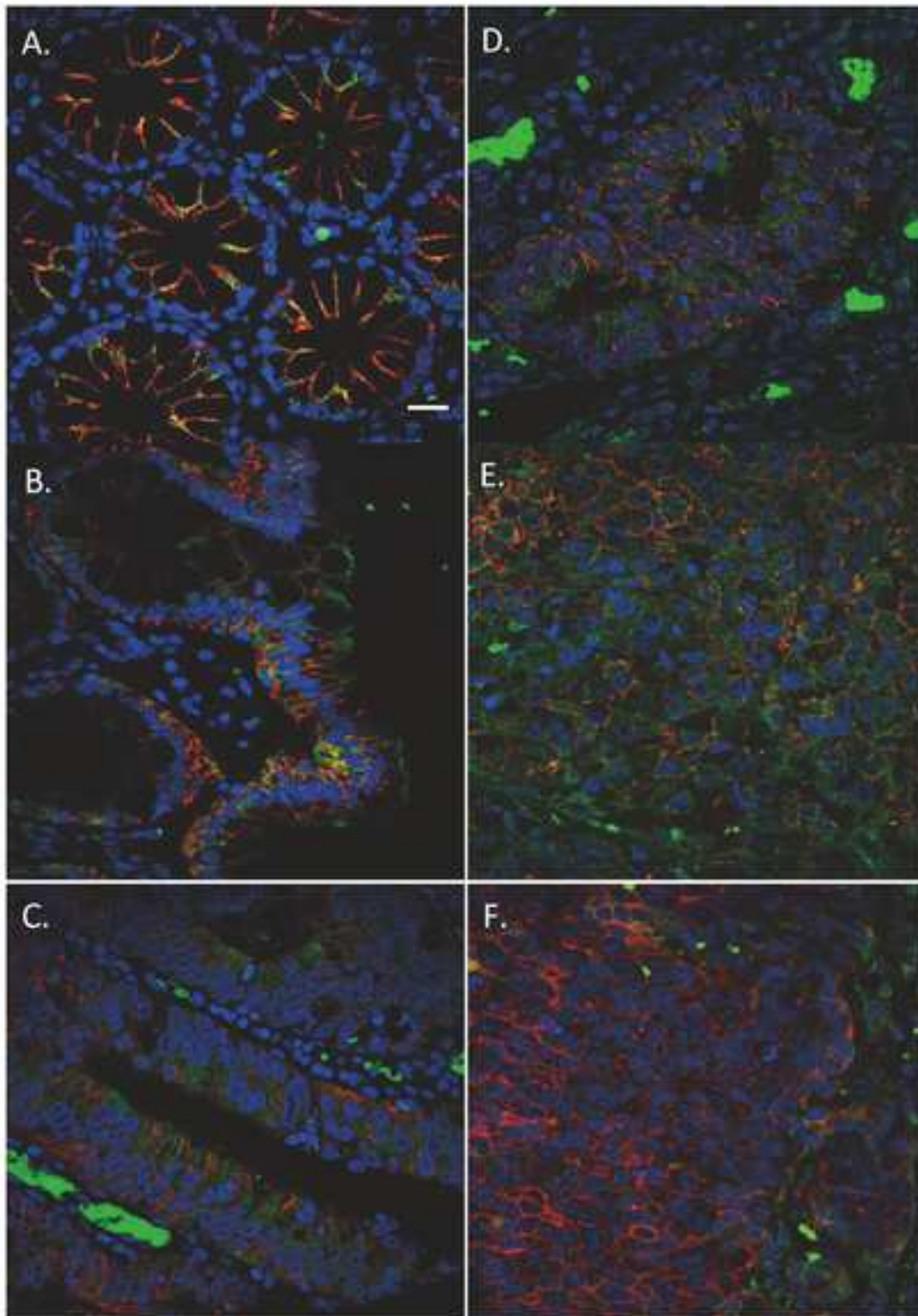
C.



D.

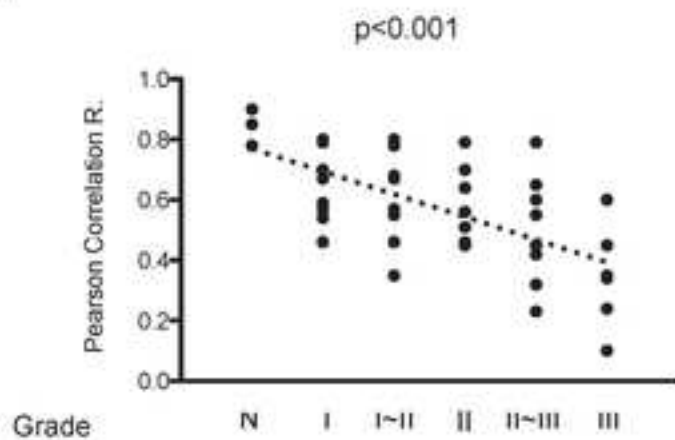


Supplemental Figure 4.

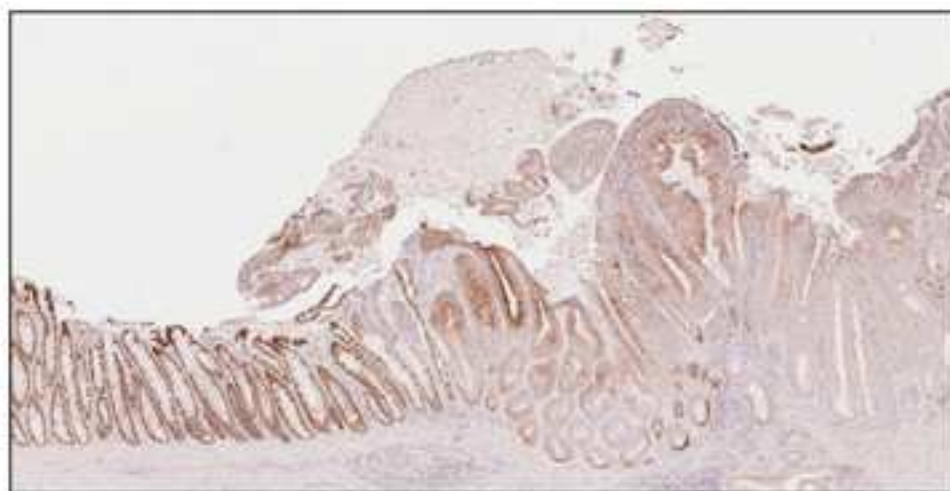


Supplemental Figure 5.

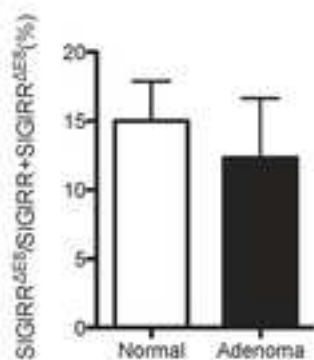
A.



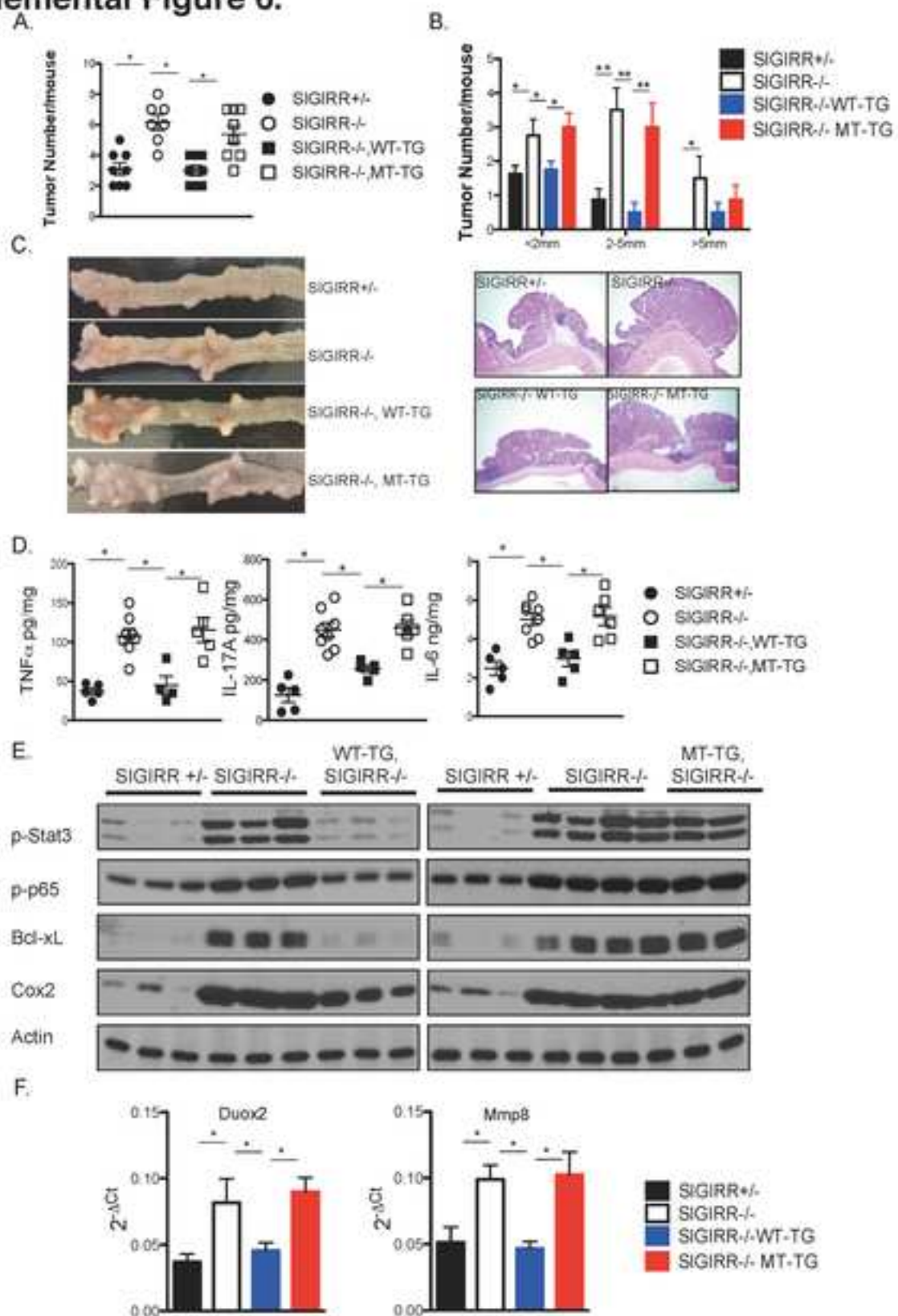
B.



C.



Supplemental Figure 6.



Supplemental Figure 7.

